Contribution from the Department of Chemistry and Materials and Molecular Research Division,
Lawrence Berkeley Laboratory, University of California, Berkeley, California 94720

Characterization of a Series of Lanthanide Amine Cage Complexes

Paul H. Smith, Zelideth E. Reyes, Chi-Woo Lee, and Kenneth N. Raymond*

The preparation and characterization of a series of encapsulated lanthanide amine complexes are discussed. The complexes of Ce, Pr, Eu, and Y with the ligand 1,9-bis(2-aminoethyl)-1,4,6,9,12,14-hexaazacyclohexadecane (referred to as L) have been prepared by using the previously described template approach (using La and Yb) involving the combination of the metal trifluoromethanesulfonate (triflate or trif) salt as the template source, 2 equiv of the tetradentate amine 2,2′,2″-tris(2-aminoethyl)amine (tren), and an excess of the formaldehyde derivative bis(dimethylamino)methane. The reduction potentials of the europium and ytterbium complexes are –0.68 and –1.37 V (vs SCE, in propylene carbonate), respectively, suggesting that this ligand imparts a large stabilization of the +3 oxidation state relative to the +2 state. An analogous lanthanum triflate complex, La(L′)(trif)$_3$ [L′ = bis((2-(2-aminoethyl)amino)ethyl)amino)methane], with one methylene bridge has been prepared and characterized by single-crystal X-ray crystallography. The structure is similar to that of the previously described dibridged complex La(L)(trif)$_3$·CH$_3$CN, and a comparison of these structures suggests possible explanations for the difficulties of obtaining the fully encapsulated lanthanide complex. The complex crystallizes in space group $P\bar{1}$ with $Z = 2$ and $a = 9.8448$ (13) Å, $b = 11.0620$ (15) Å, $c = 16.8557$ (19) Å, $\alpha = 73.456$ (9)°, $\beta = 73.684$ (10)°, and $\gamma = 70.548$ (11)°. For 6065 independent data with $F_o^2 > 3\sigma(F_o^2)$, full-matrix least-squares refinement with anisotropic thermal parameters for all non-hydrogen atoms (except disordered atoms) converged to unweighted and weighted R factors of 2.4 and 3.0%, respectively. The conductivities of acetonitrile solutions of these complexes suggest 1:1 and 1:2 electrolytes at millimolar concentrations but are highly concentration dependent, indicating that acetonitrile competes effectively with the triflate anions for the free coordination sites on the metal ion. A similar reaction produces in small yield what we believe to be a fully encapsulated ytterbium ion, Yb(L″)(trif)$_3$·CH$_3$CN [L″ = 1,4,6,9,12,14,19,21-octaazabicyclo[7.7.7]tricosane]. In contrast to the di- and monobridged complexes, this new complex does not develop a precipitate in the presence of water, which suggests that the fully encapsulated species is stable toward hydrolysis. The preparation and molecular structure of the first example of a mixed-ligand lanthanide amine complex, Pr(tren)(trien)(trif)$_3$ (trien = triethylenetetramine), is presented in an attempt to characterize the preferred geometry and appropriate bridging units for interconnecting the amine groups. The metal ion is nine-coordinate with tetradentate tren and trien ligands and one coordinated triflate anion. This complex also crystallizes in space group $P\bar{1}$ with $Z = 2$ and $a = 9.5259$ (12) Å, $b = 10.6600$ (14) Å, $c = 17.0802$ (25) Å, $\alpha = 74.284$ (12)°, $\beta = 76.914$ (11)°, and $\gamma = 85.500$ (10)°. For 2738 independent data with $F_o^2 > 3\sigma(F_o^2)$, a similar refinement converged to unweighted and weighted R factors of 3.9 and 4.6%, respectively.

Introduction

One of the fundamental properties of most lanthanide complexes is their inherent kinetic lability. The exceptions involve complexes with macrocyclic and macrobicyclic ligands that surround the metal ion in such a way as to prevent facile ligand substitution. For example, the lanthanum and cerium complexes of the macrocycle prepared from the condensation of 2,6-diacetylpyridine and ethylenediamine do not undergo metal exchange in aqueous solution, nor do they form precipitates in the presence of KOH of KF.[1] The rate constant for dissociation of the europium cryptate complexes Eu[2.2.1]$^{3+}$ and Eu[2.2.2]$^{3+}$ at pH 7 are 4.1 × 10^{-7} and 1.1 × 10^{-3} s^{-1}, respectively.[2] Two exceptional examples of complexes that are rigid in solution (on the NMR time scale) include complexes with the anionic ligands, 1,4,7,10-tetraazacyclotetradecane-1,4,7,10-tetraacetic acid (DOTA) and hydridotris(pyrazol-1-yl)borate.[3] A consequence of these unique properties is the possibility for use in a variety of applications. Such complexes have been proposed for use as NMR shift reagents for determinations of the solution structures of bound substrate molecules.[3] Another possibility is their use as T_1 relaxation agents in magnetic resonance imaging.[4] The europium and terbium complexes with the macrobicyclic ligand 2,2′,2″,9,9′,9″-bis[nitrilotri(methylene)]tris(1,10-phenanthroline) (or [phen·phen·phen]) have been proposed to have properties useful in the development of luminescent materials and of labels for biological applications.[5,6]

We have previously reported our own approach to the synthesis of a fully encapsulated lanthanide amine complex.[7,8] This approach involves a template synthesis wherein the lanthanide triflate salt, 2 equiv of tris(2-aminoethyl)amine (tren), and an excess of the formaldehyde derivative bis(dimethylamino)methane are combined to produce a macrocyclic, partial cage structure around the lanthanide ion. The structures of these compounds provide useful information about coordination number, coordination geometry, ligand conformation, and appropriate bridging lengths

for encapsulation. It was suggested that, due to its smaller size, ytterbium would be more appropriate than lanthanum for the fully encapsulated analogue.

In this work the template synthesis described above has been extended to Ce, Pr, Eu, and Y. The electrochemical properties of the complexes Ln(L)(trif)$_3$ [N = Yb and Eu] have also been characterized. The reduction potentials of these complexes in propylene carbonate suggest that the dibridged bis(tren) ligand (L) imparts a large stabilization to the +3 oxidation state relative to the +2 oxidation state. In addition, an analogous lanthanum triflate complex with one methylene bride, La(L′)(trif)$_3$ [L′ = bis((2-bis(2-aminoethyl)amino)ethyl)amino)methane], has been prepared and structurally characterized. A comparison of this structure to that of the analogous dibridged species suggests possible explanations for the difficulties of obtaining the fully encapsulated lanthanide complex. A mixed amine complex of praseodymium, Pr(tren)(trien)(trif)$_3$, has also been prepared and structurally characterized as a potential precursor to new types of encapsulation complexes. Finally, we have prepared in small yield what we believe to be a fully encapsulated ytterbium complex, Yb(L″)(trif)$_3$·CH$_3$CN [L″ = 1,4,6,9,12,14,19,21-octaazabicyclo[7.7.7]tricosane]. In contrast to the previously reported dibridged complexes, this new complex shows no evidence for decomposition in water, and this suggests that the fully encapsulated

(1) Backer-Dirks, J. D. J.; Gray, C. J.; Hart, F. A.; Hursthouse, M. B.; Schoop, B. D. *J. Chem. Soc., Chem. Commun.* **1979**, 744. De Cola, L.; Smailes, D. L.; Vallarino, L. M. *Inorg. Chem.* **1986**, *25*, 1729–1732.
(2) Yee, E. L.; Gansow, O. A.; Weaver, M. J. *J. Am. Chem. Soc.* **1980**, *102*, 2278.
(3) Spirlet, M.-R.; Rebizant, J.; Desreaux, J. F.; Locin, M.-F. *Inorg. Chem.* **1984**, *23*, 359. Desreaux, J. F. *Inorg. Chem.* **1980**, *19*, 1319.
(4) Budinger, T. F.; Margulis, A. R. *Medical Magnetic Resonance Imaging and Spectroscopy, a Primer*; Society of Magnetic Resonance in Medicine: Berkeley, CA, 1986.
(5) Rodriguez-Ubis, J.-C.; Alpha, B.; Plancherel, D.; Lehn, J.-M. *Helv. Chim. Acta* **1984**, *67*, 2264.
(6) Alpha, B.; Lehn, J.-M.; Mathis, G. *Angew. Chem., Int. Ed. Engl.* **1987**, *26*, 266.
(7) Eigenbrot, C. W., Jr.; Raymond, K. N. *Inorg. Chem.* **1982**, *21*, 2867.
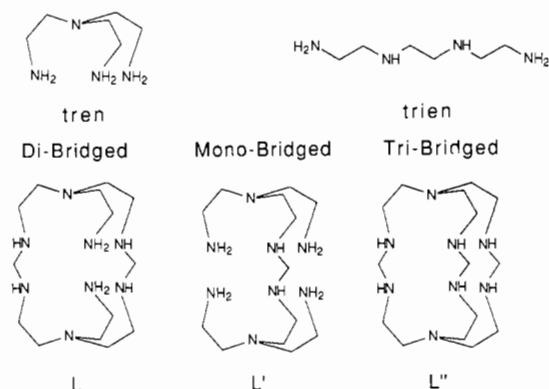(8) Smith, P. H.; Raymond, K. N. *Inorg. Chem.* **1985**, *24*, 3469.

---

*To whom correspondence should be addressed at the Department of Chemistry, University of California.

Figure 1. Illustrations of the various amine ligands discussed in this work.

species is stable toward hydrolysis. The ligands discussed in this work are illustrated in Figure 1.

Experimental Section

All manipulations of moisture sensitive compounds were accomplished with Schlenk and syringe techniques and the use of a nitrogen-atmosphere glovebag or an argon-filled glovebox.[9] Elemental analyses were performed by the Microanalytical Laboratory, University of California, Berkeley, CA. Fast atom bombardment mass spectra were obtained at the Mass Spectrometry Laboratory at the University of California, Berkeley, CA. The lanthanides were determined by the weight of the residue from the sulfur analysis, assuming the residue was LnF_3.[10] Infrared spectra were obtained on a Perkin-Elmer 597 spectrophotometer and a Nicolet 5-DXB FTIR (Nujol mulls). NMR spectra were obtained in deuteriated acetonitrile on the University of California, Berkeley, CA, 200 MHz FT-NMR instrument by using the CD_2HCN quintet at δ 1.93 (for ^1H spectra) as the reference (unless otherwise stated). The ^{13}C spectra are also referenced to CD_3CN at δ 1.3. All δ values are relative to TMS. Deuteriated acetonitrile (obtained from Aldrich) was stored over 3-Å molecular sieves in a desiccator containing Drierite.

Materials. Acetonitrile (CH_3CN) was distilled from phosphorous pentoxide, tetrahydrofuran (THF) from potassium, diethyl ether (Et_2O) from calcium hydride, toluene from sodium, and pyridine from potassium hydroxide. All solvents were stored under an inert atmosphere, and toluene was stored over 3-Å molecular sieves. The ligand, tren, was extracted from crude triethylenetetramine[11] and distilled from Na, or it was used as obtained from Aldrich. Trifluoromethanesulfonic acid was used as obtained from Aldrich or Aesar. Lanthanide oxides were obtained from Brewer or Apache. Bis(dimethylamino)methane was prepared by the addition of paraformaldehyde to an aqueous solution of dimethylamine, followed by distillation through a 30-cm Vigreux column and subsequent distillation from Na (bp 80–83 °C at 1 atm, 61% yield, 1 H NMR ($CDCl_3$): δ 1.93, s, area = 1; δ 1.45, s, area = 6), or it was used as obtained from Aldrich.

The lanthanide triflate salts [Ln(trif)$_3$; Ln = La, Pr] were prepared by the addition of trifluoromethanesulfonic acid to a suspension of the oxide in water. Excess oxide was added to bring the pH to 4–5. The undissolved oxide was then removed by filtration, and the water was evaporated on a rotary evaporator. The resulting solid was dried at 160–200 °C for $\simeq$24 h under vacuum and used without further purification. The europium and ytterbium salts were prepared similarly except that the reaction mixture was refluxed for approximately 1 h before filtering. (*Caution!* The perchlorate compounds can result in highly explosive materials. Their use should be replaced by the procedure described here.) Europium and yttrium triflates were also obtained from Aesar and used after drying overnight at 100 °C and 0.01 mmHg in a vacuum oven. The cerium(III) triflate salt was prepared by the addition of trifluoromethanesulfonic acid to an aqueous solution of cerium trichloride (prepared by dissolving $CeCl_3 \cdot XH_2O$, Apache) and subsequent evaporation of water and hydrochloric acid by rotoevaporation. The metal triflate salts used in the following syntheses were not rigorously dry, as determined from the OH stretch in the infrared spectra. The europium salt was recrystallized from acetonitrile and dried at 100 °C at 0.01 mmHg for 24 h. Anal. Found (calcd) for $Eu_1C_3S_3O_9F_9$: C, 6.36 (6.01); H, 0.26 (0.0); N, 0.03 (0.0); S, 16.20 (16.05). The ytterbium salt was recrystallized from THF/Et_2O ($\simeq$1/1) at room temperature and

dried for 48 h at 100 °C and 0.01 mmHg. Anal. Found (calcd) for $Yb_1C_3S_3O_9F_9$: C, 5.90 (5.81); H, 0.11 (0.0); N, 0.05 (0.0); S, 15.27 (15.51). Infrared (cm^{-1}): 3511, br; 1633; 1460; 1231, br; 1050, br; 802; 774, w; 722, w; 645, br; 582; 518.

Electrochemistry. The cyclic voltammograms were measured by using a Princeton Applied Research potentiostat/galvanostat (Model 173) and a Universal programmer (Model 175). The pulse polarograms were measured by using a Princeton Applied Research polarographic analyzer (Model 174A). Propylene carbonate was obtained from Alfa Products (99%), distilled from 3-Å molecular sieves under vacuum, and stored under nitrogen. Tetraethylammonium perchlorate (Aldrich, reagent grade) was recrystallized from ethanol and dried before use. Acetonitrile was distilled immediately before use from phosphorous pentoxide through a 60-cm Vigreux column and stored under nitrogen. Lithium triflate was obtained from Aldrich (97%), recrystallized from acetonitrile, dried under vacuum, and stored under nitrogen. Solutions were purged with and handled uner argon. The cyclic voltammetry was done in a one-compartment cell, with a hanging mercury drop as the working electrode (HMDE), a platinum wire as the counter electrode, and a saturated calomel electrode (SCE) as the reference electrode.[12] Normal- and differential-pulse polarography were done in the same cell with a dropping-mercury working electrode (DME). The propylene carbonate solutions were 3 mM in Ln(L)$^{3+}$ and 0.1 M in tetraethylammonium perchlorate. The acetonitrile solutions were 2–3 mM in Ln(L)$^{3+}$ and 0.3 M in lithium triflate. Experiments were conducted at laboratory temperature, 22 ± 2 °C. Details specific to the experiments are provided in the appropriate figure captions.

Conductivity. Conductivity measurements were performed in acetonitrile (freshly distilled from phosphorous pentoxide) by using a Barnstead Model PM-70CB and B-1 cell with a cell constant of 0.08 cm^{-1} (determined in aqueous KCl solution[13]). The electrodes were lightly platinized with a Model No. 3139 platinizing kit with YSI3140 platinizing solution (Yellow Springs Instrument Co., Inc.). Measurements were performed at ambient temperature (21 ± 1 °C) under nitrogen purge. The specific conductance of the pure solvent was 5.4×10^{-7} cm^{-1} Ω^{-1}.

Triethylenetetramine (trien). To 26 g of trien·XH$_2$O (Aldrich, 99%) was added $\simeq$60 mL of water and 56 g of KOH. This mixture was warmed to melt the trien hydrate and was subsequently extracted three times with $\simeq$100-mL portions of toluene. The combined toluene layers were concentrated by rotoevaporation to give crude trien (20 g). This clear liquid was dried over sodium metal for $\simeq$2 days and then distilled under vacuum. The major fraction (16 g) was redistilled (93–98 °C at 0.05 mmHg) to give 14 g of a clear colorless liquid, which was used without further purification.

La(tren)$_2$(trif)$_3$. La(trif)$_3$ (5.2 g, 8.8 mmol) was weighed quickly in air into a dry Schlenk flask equipped with a stir bar, and THF (50 mL) was added via cannula. Upon addition of tren (2.6 mL, 18 mmol), the solid dissolved to give a clear solution, which was subsequently heated to reflux ($\simeq$1 min). Upon slow addition of Et_2O a precipitate formed which redissolved upon stirring. Et_2O was added slowly via cannula until the solid would not redissolve upon warming. A few drops of THF were added to redissolve the solid, and the solution was allowed to stand at room temperature for 1 h and then at −20 °C overnight (THF/Et_2O $\simeq$ 3/1). The resulting crystalline solid was collected by inert-atmosphere filtration, washed once with a 1/1 mixture of THF/Et_2O and then dried at 70 °C at 0.5 mmHg overnight (5.2 g, 67% yield). Anal. Found (calcd) for $LaC_{15}H_{36}N_8O_9S_3F_9$: La, 14.9 (15.8); C, 20.59 (20.50); H, 4.52 (4.13); N, 12.08 (12.75); S, 10.10 (10.95). (The analytical sample was handled in air and is quite hygroscopic.) Infrared: See Table I. NMR: ^1H, δ 2.8 (mult); ^{13}C, δ 60.1, 41.3 (CD_3CN reference set at δ 1.3).

Eu(tren)$_2$(trif)$_3$·CH$_3$CN. The preparation of this compound was similar to the preparation of the analogous lanthanum complex except that the compound was crystallized from a $\simeq$1:1 mixture of acetonitrile/diethyl ether (yield $\simeq$ 50%). Anal. Found (calcd) for $EuC_{15}H_{36}N_8O_9S_3F_9$·$CH_3CN$: C, 21.55 (21.89); H, 4.58 (4.22); N, 13.26 (13.52); S, 10.46 (10.31). Infrared: See Table I. ^1H NMR: δ 19.2 (br), 4.2, 2.77 (t), 2.63 (t), −3.4 (br), −6.7.

La(L')(trif)$_3$. La(tren)$_2$(trif)$_3$ (5.5 g, 6.3 mmol) was dissolved in $\simeq$50 mL of acetonitrile in a 250-mL round-bottom flask equipped with a magnetic stir bar and sealed under nitrogen. The resultant, slightly cloudy solution was heated to reflux and then bis(dimethylamino)methane (1.0 mL, 7.3 mmol) was added via syringe. The mixture was

(9) Shriver, D. F. *The Manipulation of Air-Sensitive Compounds*; McGraw-Hill: New York, 1969.
(10) Roberts, J. E.; Bykowski, J. S. *Thermochim. Acta* **1978**, *25*, 233.
(11) Forsberg, J. H.; Kubik, T. M.; Moeller, T.; Gucwa, K. *Inorg. Chem.* **1971**, *10*, 2656.

(12) The potentials in acetonitrile were also measured relative to a Ag/AgNO$_3$ reference, and the values were consistently 0.23 V more negative compared to SCE.
(13) Vogel, A. I. *A Textbook of Quantitative Inorganic Analysis*, 3rd ed.; Longman Tender: 1962; pp 972–974.

Table I. Infrared Data (cm^{-1}) for Lanthanide Amine Triflate Complexes[a]

Latn2	Eutn2	Ptntn	LaL	LaL'	CeL	PrL	EuL	YbL	YbL''	YL
3318	3320	3335	3346	3342	3348	3347	3352	3326	3365	3537
3278	3279	3283	3297	3331	3298	3296	3345	3285	3325	3329
3181	3178	3276	2250	3306	1733	1734	3302	3261	3310	3281
1610	2251	3187	1605	3289	1608	1609	3275	2251	3285	3262
1461	1613	1603	1465	1613	1466	1464	1466	1585	3245	1734
1377	1462	1464	1378	1594	1376	1376	1377	1464	2250	1583
1260	1377	1458	1260	1466	1307	1306	1300	1378	1595	1487
1167	1257	1377	1162	1378	1169	1284	1288	1355	1308	1465
1032	1168	1327	1108	1308	1123	1238	1242	1319	1457	1377
985	1090	1315	1082	1287	1110	1222	1221	1255	1373	1365
971	1074	1279	1028	1242	1081	1168	1187	1214	1311	1319
904	1033	1252	987	1224	1057	1124	1159	1160	1298	1273
891	992	1208	949	1160	990	1111	1115	1124	1281	1254
879	978	1156	895	1033	946	1080	1090	1108	1255	1239
861	909	1117	874	995	925	1056	1057	1095	1233	1215
852	896	1072	806	984	896	989	1032	1057	1217	1163
799	881	1030	764	950	876	949	992	1029	1168	1122
760	863	995	741	885	836	898	960	971	1140	1110
742	801	964	639	849	820	877	876	953	1124	1093
723	759	899	593	800	761	837	820	928	1103	1081
641	746	883	575	763	742	820	743	916	1079	1067
574	723	869	518	742	636	762	639	901	1028	1055
517	641	852	475	639	589	744	604	871	1022	1030
492	575	826		575	576	591	571	835	981	1006
	575	796		519	563	575	519	798	962	987
	517	760		497	519	565	501	740	937	964
	505	745		474	477	519	480	638	895	949
		723			435	485		575	842	911
		639						517	826	898
		576							630	868
		518								832
		486								761
		459								745
										723
										637
										575
										575
										517
										497

[a] Latn2 = La(tren)$_2$(trif)$_3$, Eutn2 = Eu(tren)$_2$(trif)$_3$·CH$_3$CN, Ptntn = Pr(tren)(trien)(trif)$_3$, LaL = La(L)(trif)$_3$·CH$_3$CN, LaL' = La(L')(trif)$_3$, CeL = Ce(L)(trif)$_3$, PrL = Pr(L)(trif)$_3$, EuL = Eu(L)(trif)$_3$, YbL = Yb(L)(trif)$_3$·CH$_3$CN, YL = Y(L)(trif)$_3$, YbL'' = Yb(L'')(trif)$_3$·CH$_3$CN.

refluxed for 30 min, and the solvent was removed under vacuum. The resulting off-white solid was dried at 70 °C and 0.1 mmHg overnight and then extracted two times with 25-mL portions of hot THF. The THF washes were collected by Schlenk filtration through a Celite-packed glass frit to give a clear yellowish solution, which was allowed to cool to room temperature and subsequently was cooled to −20 °C overnight. The resulting crystalline solid was collected by filtration and dried at 70 °C at 0.1 mmHg overnight (1.4 g, 1.6 mmol). The THF-insoluble portion from above was dissolved in ≃40 mL of acetonitrile and filtered through a Celite-packed frit, and the volume was reduced under vacuum to give a clear yellowish solution (≃10 mL). Upon cooling (−20 °C, 3–4 h), some crystalline solid formed, which was collected by filtration and similarly dried (0.81 g, 0.91 mmol). The mother liquors were evaporated and dried as above (0.91 g, 1.0 mmol). The above three samples had identical NMR spectra, and the crystalline solid from acetonitrile was used for elemental analysis (total yield ≃ 54%). Crystals suitable for single-crystal X-ray diffraction were obtained from an acetonitrile/diethyl ether (≃5/1) mixture. Anal. Found (calcd) for LaC$_{16}$H$_{36}$N$_8$O$_9$S$_3$F$_9$: C, 21.40 (21.58); H, 4.01 (4.08); N, 12.40 (12.58); S, 10.36 (10.80). Infrared: See Table I. NMR: ^{1}H, δ 4.0 (trip), 3.47 (trip, br), 3.1 (mult), 2.7 (mult), 2.6 (mult); ^{13}C, δ 62.7, 60.6, 59.0, 56.9, 46.6, 41.05, 40.96. Positive ion FAB MS: molecular ion = [La-(L')(trif)$_2$]$^+$, 741; major ions observed at *m/z* 743, 753, 755, 767.

La(L)(trif)$_3$. This complex was prepared as described previously.[8] Infrared: See Table I. NMR: ^{1}H, δ 4.1 (mult), 3.8 (br), 3.0 (mult), 2.75 (mult), 2.5 (mult); ^{13}C, δ 63.0, 59.4, 58.8, 55.9, 47.3, 44.8, 40.6. Positive ion FAB MS: molecular ion = [La(L)(trif)$_2$]$^+$ at *m/z* 753 (with appropriate isotope distribution).

Yb(L)(trif)$_3$. This complex was prepared as described previously.[8] It can be obtained in a manner similar to the preparation of La(L)(trif)$_3$. A typical yield in this case is 30–40%. When the ytterbium bis(tren) complex is isolated first and used as the starting material, the yield is 67%. Infrared: See Table I. ^{1}H NMR: δ 95 (v br), 65 (v br), 45 (v br), 37, 29, 20, 12, 7 (mult), −6, −12, −21, −32, −43, −58, −78, −100 (v

br) −144 (v br), −198 (v br). Positive ion FAB MS: molecular ion = [Yb(L)(trif)$_2$]$^+$ at *m/z* 788 (with appropriate isotope distribution).

Ce(L)(trif)$_3$. The preparation of this compound is similar to that of La(L)(trif)$_3$ (yield ≃ 50–60%). The analytical sample was dried at 70 °C overnight at 0.1 mmHg. Anal. Found (calcd) for CeC$_{17}$H$_{36}$N$_8$O$_9$S$_3$F$_9$: C, 22.93 (22.59); H, 4.04 (4.02); N, 12.18 (12.40); S, 10.54 (10.64). Infrared: See Table I. ^{1}H NMR: δ 19.05 (area = 1), 18.73 (area = 1), 11.67 (area = 1), 11.21 (area = 1), 10.71 (area = 2), 9.76 (area = 1), 6.81 (area = 2), 3.08 (area = 1), 2.23 (area = 1), 1.32 (area = 1), 0.80 (area = 1), −2.08 (area = 1), −4.10 (area = 1), −5.87 (area = 1), −8.65 (area = 1), −12.52 (area = 1). Positive ion FAB MS: molecular ion = [Ce(L)(trif)$_2$]$^+$ at *m/z* (with appropriate isotope distribution).

Pr(L)(trif)$_3$. The preparation of this compound is similar to that of La(L)(trif)$_3$ (yield ≃ 62%). Anal. Found (calcd) for PrC$_{17}$H$_{36}$N$_8$O$_9$S$_3$F$_9$·CH$_3$CN: Pr, 13.9 (14.9); C, 24.55 (24.13); H, 4.22 (4.16); N, 13.44 (13.33); S, 9.30 (10.17). Infrared: See Table I. ^{1}H NMR: δ 32.84, 30.79, 23.06, 21.95, 21.22, 16.90, 13.43, 9.99, 8.63, 4.52, 3.93, 2.05, −0.27, −3.22, −9.57, −9.86, −18.94, −28.21. Positive ion FAB MS: molecular ion = [Pr(L)(trif)$_2$]$^+$ at *m/z* 755 (with appropriate isotope distribution).

Eu(L)(trif)$_3$. Eu(tren)$_2$(trif)$_3$ (2.3 g, 2.5 mmol) was dissolved in ≃50 mL of acetonitrile in a large Schlenk flask with a magnetic stir bar. After the solution was heated to reflux, bis(dimethylamino)methane (1.0 mL, 7.3 mmol) was added via syringe. After the mixture was refluxed for 6$^1/_2$ h the solvent was removed under vacuum to give a yellowish solid, which was dried overnight at 70 °C and 0.05 mmHg. This solid was recrystallized from ≃50 mL of acetonitrile by the addition of 5–10 mL of diethyl ether and subsequent cooling (≃30% isolated yield). Anal. Found (calcd) for EuC$_{17}$H$_{36}$N$_8$O$_9$S$_3$F$_9$·$^1/_2$CH$_3$CN: C, 23.04 (23.08); H, 3.87 (4.04); N, 12.22 (12.71); S, 9.94 (10.28). Infrared: See Table I. ^{1}H NMR: δ 26.19 (mult), 25.70, 17.01, 15.58, 14.77, 12.44 (mult), 3.00, −0.93, −0.99, −1.05, −2.38, −6.37, −6.39, −8.36, −8.43, −9.34, −9.36, −9.69, −9.75, −10.09, −10.15, −14.90 (mult), −15.99, −16.05, −17.50, −17.58,

−19.41, −19.47, −21.25 (br), −25.52, −25.58. Positive ion FAB MS: molecular ion = [Eu(L)(trif)$_2$]$^+$ at m/z 767 (with appropriate isotope distribution).

Y(L)(trif)$_3$. This compound was isolated in an attempt to prepare the triply bridged complex. Y(trif)$_3$ (2.1 g, 3.8 mmol) was placed in a $^3/_4$ in. diameter, thick-walled glass tube, and ≃ 5 mL of pyridine was added. Tren (1.1 g, 7.5 mmol) and bis(dimethylamino)methane (2.0 mL, 15 mmol) were added via syringe. Before sealing, the mixture was heated to reflux with a needle vent through a septum seal. The vent was removed and the tube and contents were frozen in liquid nitrogen. The tube was flame sealed and then placed in an oil bath at ≃150 °C for 30 min. The solution turned black but remained homogeneous. The tube was frozen in liquid nitrogen and then scored and broken at the top. Upon warming, the contents were poured into a 250-mL Schlenk flask and the solvent was removed under vacuum to give a sticky brown solid. This solid was extracted with ≃ 20 mL of THF. To the decanted THF extract was added ≃5 mL of diethyl ether, at which point an oily precipitate began to form on the walls of the flask. The solution was decanted again and the mother liquors were cooled at ≃ 5 °C overnight. The resulting crystalline material was collected by decantation and dried overnight at 70 °C and 0.05 mmHg (yield ≃ 3–5%). Anal. Found (calcd) for YC$_{17}$H$_{36}$N$_8$O$_9$S$_3$F$_9$: C, 24.32 (23.95); H, 4.29 (4.26); N, 13.11 (13.14); S, 10.83 (11.28). Infrared: See Table I. NMR: ^{1}H, δ 4.1 (mult), 3.9 (br), 3.25 (mult), 3.1 (mult), 2.9 (br), 2.8 (mult), 2.6, 2.55; ^{13}C; δ 59.54, 59.14, 55.85, 49.92, 46.35, 46.29, 41.79, 41.13. Positive ion FAB MS: molecular ion = [Y(L)(trif)$_2$]$^+$ at m/z 703.

Pr(tren)(trien)(trif)$_3$. Pr(trif)$_3$ was suspended in ≃50 mL of acetonitrile in a 250-mL Schlenk flask equipped with a magnetic stir bar under a nitrogen atmosphere. Then tren (2.0 mL, 13 mmol) and trien (2.0 mL, 13 mmol) were added simultaneously via two syringes. Upon addition of ≃70 mL more acetonitrile via cannula most of the solid dissolved. This solution was heated to reflux briefly and then clarified by filtration through a glass frit. The volume of the resulting light green clear solution was reduced under vacuum to ≃20 mL and cooled to −20 °C for ≃6 h. The solution was decanted from the resulting crystalline solid, and this solid was dried under vacuum at room temperature overnight (6.6 g, 7.5 mmol). The mother liquors were cooled overnight, and the resulting solid was collected by decantation and dried similarly (1.7 g, 1.9 mmol, overall yield = 72%). Crystals suitable for single-crystal X-ray diffraction were obtained from acetonitrile by allowing a warm saturated solution to cool to room temperature overnight. Anal. Found (calcd) for PrC$_{15}$H$_{36}$N$_8$O$_9$S$_3$F$_9$: C, 20.69 (20.46); H, 4.13 (4.12); N, 12.59 (12.73); S, 9.73 (10.92). Infrared: See Table I. ^{1}H NMR: δ 21.7, 19.5, 18.8, 17.2, 14.9, 13.6, 12.4, 11.4, 10.6, 9.6, 8.3, 7.5, 7.1, 3.6, 3.52, 3.49, −0.5, −1.2, −11.2, −19.3, −24.3.

Yb(L″)(trif)$_3$·CH$_3$CN. Yb(trif)$_3$ (4.0 g, 6.5 mmol) was weighed quickly (in air) into a large Schlenk flask equipped with a stir bar, and the flask was flushed three times with N$_2$. When 30–40 mL of freshly distilled acetonitrile was added and the mixture was heated to 80–90 °C, some of the triflate salt dissolved. Then tren (1.9 mL, 13 mmol) was added with a syringe, at which point most of the triflate salt dissolved. To this slightly cloudy solution was added bis(dimethylamino)methane (8.7 mL, 64 mmol) with a syringe. The mixture was refluxed under a nitrogen atmosphere for 25 h. The resulting dark red-brown mixture was cooled to room temperature, and the solvent was removed under vacuum while the solution was warmed with a heat gun. The resulting brownish solid was dried overnight at room temperature under vacuum. It was then dissolved in 5–10 mL of acetonitrile, and then toluene was added (via cannula) until a dark oil formed. After addition of acetonitrile to redissolve the oil, the clear dark brown solution was cooled to −20 °C. After 3 days a crystalline mass had formed, which was identified as the dibridged bis(tren) complex, Yb(L)(trif)$_3$·CH$_3$CN. The mother liquors were decanted into two separate vials, which were then sealed with septa under nitrogen (total volume ≃25–30 mL). After approximately 2 months at room temperature a solid had formed in these vials. The mother liquors were decanted, and the solids were combined and recrystallized from ≃5 mL of acetonitrile by cooling to −20 °C. The resulting fine white precipitate was collected by filtration, washed with toluene, and dried briefly by passing nitrogen over the sample. This sample was recrystallized again from acetonitrile and submitted for analysis (yield ≃3–5%). Anal. Found (calcd) for YbC$_{20}$H$_{39}$N$_9$O$_9$S$_3$F$_9$: C, 24.45 (24.27); H, 3.89 (3.97); N, 12.35 (12.74); S, 9.49 (9.72); Yb, 16.0 (17.48). Infrared (NaCl): See Table I. ^{1}H NMR in CD$_3$CN: δ 97.6, 95.2, 80.6, 79.0, 75.6, 66.2, 57.5 (br), 44.0, 43.3, 41.6, 38.5, 36.1, 34.8, 32.4, 30.1, 28.2, 27.2, 25.4, 24.3, 21.4, 19.5, 17.9, 15.8, 14.4, 11.8, 9.3, 7.9, 6.9, 6.2, −6.1, −7.5, −8.3, −10.8, −14.5, −16.9, −17.8, −22.6, −28.9, −30.1, −36.1, −40.7, −41.8, −44.5, −49.4, −49.7, −52.5, −56.6, −58.6, −66.2, −68.9, −79.4, −81.6, −110. ^{1}H NMR in D$_2$O: δ 42.3, 33.1, 28.4, 25.5, 23.8, 20.5, 18.7, 10.1, 5.7, −1.4, −4.9, −13.4, −18.9, −21.1, −24.9, −25.5, −41.4, −42.3, −53.4, −61.6, −64.1, −68.7, −73.7. Positive ion FAB MS:

Table II. Data Collection, Solution, and Refinement Parameters for La(L′)(trif)$_3$ and Pr(tren)(trien)(trif)$_3$

	LaC$_{16}$H$_{36}$N$_8$F$_9$O$_9$S$_3$	PrC$_{15}$H$_{36}$N$_8$F$_9$O$_9$S$_3$
mol wt	890.6	880.6
space group	$P\bar{1}$	$P\bar{1}$
a, Å	9.8448 (13)	9.5259 (12)
b, Å	11.0620 (15)	10.6600 (14)
c, Å	16.8557 (19)	17.0802 (25)
α, deg	73.456 (9)	74.284 (12)
β, deg	73.684 (10)	76.914 (11)
γ, deg	70.548 (11)	85.500 (10)
V, Å^3	1623.6 (3)	1626.0 (8)
Z	2	2
D_{obs}, g cm^{-3}	1.77	1.80
D_{calc}, g cm^{-3}	1.82	1.80
cryst dimens, mm	0.09 × 0.27 × 0.32	0.06 × 0.1 × 0.3
μ, cm^{-1}	16.1	17.84
abs range T_{max}	0.88	1.0
abs range T_{min}	0.72	0.96
decay, %	18.1	30
2θ range, deg	3–55	2–45
tot. no. of data measd	14847	8456
no. of data measd with $I > 3\sigma(I)$	12432	6035
total no. of indep data	7429	4235
no. of indep data with $F_o^2 > 3\sigma(F_o^2)$	6065	2738
averaging $R(I)$, %	2.1	4.2
averaging $R(F)$, %	1.5	3.2
refinement R, %	2.4	3.9
refinement R_w, %	3.0	4.6
GOF	1.156	1.327
p factor	0.03	0.04
no. of params	460	415
extinction coeff g	none	none
max peak on ΔF map, e Å^{-3}	0.67 near F9	1.08 near S1
temp, °C	−110	+25

m/z calculated for [Yb(L″)(trif)$_2$·CH$_3$CN]$^+$, 841 (with appropriate isotope distribution pattern).

Data Collection, Solution, and Refinement. The following information pertains to both structures, and details appear in Table II. Crystals were mounted in glass capillaries in an inert-atmosphere drybox. The space groups were suggested by precession photographs and confirmed by successful refinements. Cell constants were determined and intensity data were collected on a Nonius CAD-4 automated diffractometer with κ geometry using the θ–2θ scan mode[14] (monochromated Mo Kα radiation, λ = 0.71073 Å[15]). Data (±h,±k,±l) were collected while three intensity standards were monitored every 2 h of X-ray exposure time and three orientation standards were checked every 250 reflections. The structures were solved with heavy-atom techniques. Hydrogens were placed in idealized positions with isotropic thermal parameters based on their parent carbon and nitrogen atoms and were not refined.[16] Full-matrix least-squares refinements were employed for the reflections with $F_o^2 > 3\sigma(F_o^2)$.

Results and Discussion

Synthesis and Characterization. The synthesis of Ln(L)(trif)$_3$ (Ln = Ce, Pr, Eu, Y) is similar to that above and in a previous paper.[8] The synthesis of La(L′)(trif)$_3$ is similar except that only 1 equiv of the formaldehyde reagent is added, and the reaction is heated at reflux for only $^1/_2$ h, compared to overnight for the dibridged analogue. A similar attempt was made to prepare Eu(L′)(trif)$_3$, but only the dibridged complex, Eu(L)(trif)$_3$, could be isolated, and the NMR and FAB mass spectra revealed no

(14) For details regarding data reduction and processing, scattering factor tables, and the program ORTEP, please refer to: Eigenbrot, C. W., Jr.; Raymond, K. N. *Inorg. Chem.* **1982**, *21*, 2653. Atomic scattering factors were obtained from: *International Tables for X-Ray Crystallography*; Kynoch: Birmingham, England, 1974; Vol. IV, Tables 2.2b and 2.3.1.

(15) Kα is the intensity-weighted average of Kα$_1$ and Kα$_2$.

(16) The hydrogen atom isotropic thermal parameters were calculated by multiplying the parent atom isotropic equivalent thermal parameter by a constant value. For La(L′)(trif)$_3$ the value was 1.1, and for Pr(tren)(trien)(trif)$_3$ it was 1.3.

evidence for the monobridged version, Eu(L')(trif)$_3$. This observation suggests that the monobridged europium complex is more reactive toward bis(dimethylamino)methane than is the lanthanum complex, La(L')(trif)$_3$.

The praseodymium mixed-amine complex, Pr(tren)(trien)(trif)$_3$, was originally isolated from an attempt to make the bis(trien) complex. The batch of trien used in this case was technical grade, which contains approximately 10% tren. The yield of the mixed complex is on the order of 70% when equal amounts of the pure ligands are used. This raises the question of what actually exists in solution. It is possible that the solubility of the mixed complex is such that it is the first of the three possible complexes in solution that crystallizes. An attempt was made to prepare a bridged analogue by adding bis(dimethylamino)methane to a solution of the complex under conditions similar to those used in the preparation of La(L)(trif)$_3$ described previously. At least 50% of the starting material was recovered from the reaction mixture, and the ^{1}H NMR spectrum showed evidence for starting material and for Pr(L)(trif)$_3$ (10–20%) only. This suggests that the mixed complex reacts very slowly or not at all with the formaldehyde derivative. In the solid state the triflate anion is coordinated in the center of the four primary amines that would be most likely to react, and the observed slow reactivity may be due to steric hindrance from this triflate anion.

The fully encapsulated complex, Yb(L'')(trif)$_3$·CH$_3$CN, was prepared by using a large excess of coupling reagent and a long reaction time. It was formed in low yield and was isolated from a mixture of the dibridged complex and other impurities by crystallization.

The positive ion fast-atom-bombardment mass spectra have proven to be the simplest and most definitive means of characterization. The observed molecular ion peaks correspond to the +1 ions (loss of one triflate anion), and the isotope distribution patterns confirm the presence of the metal ion in most cases. The FAB mass spectrum of La(L')(trif)$_3$ is the exception to this rule. The expected mass of m/z 741 is not observed, and the major ions observed are at m/z 743, 753, 755, and 767. The m/z 753 ion is the principal ion observed for the lanthanum dibridged complex. The FAB mass spectrum of Yb(L'')(trif)$_3$·CH$_3$CN shows a parent ion of m/z 841, which corresponds to a ytterbium bis(tren) complex with three methylene bridges, two triflates (making it a singly charged cation), and one acetonitrile. The calculated isotope distribution matches quite well, confirming the presence of the ytterbium ion. The elemental analysis for this complex is quite good, but the difference between 19 and 20 carbon atoms is only about 1% of the total weight of the complex. The acetonitrile that is used in the calculation of the analysis and the FAB mass spectrum is seen in the IR spectrum as a weak sharp band at 2250 cm^{-1}. The N–H stretch region of the IR is significantly different from that of Yb(L)(trif)$_3$, showing five sharp bands as opposed to four.

The NMR spectra of these complexes are typically quite complex; however, they do provide some information about the solution structures. The ^{13}C NMR spectra of the diamagnetic complexes La(L)(trif)$_3$ and La(L')(trif)$_3$ reveal details about the symmetry of these complexes in solution. The spectrum of the dibridged complex has seven peaks between 65 and 40 ppm, and there are 14 carbon atoms in the complex (excluding the triflate carbons, which are not observed but would be expected to be much further downfield). This suggests that this complex has a C_2 axis in solution (on the NMR time scale) and is consistent with the approximate C_2 axis observed in the solid state.[8] It is entirely possible that the nonbridged primary amine arms are fluxional in acetonitrile solution, but the configuration of the secondary amines probably remains intact, since it would require a concerted process whereby the four coordinated amines undergo proton transfer and inversion virtually simultaneously. The fact that this type of averaging is not observed as a simplification in the NMR spectra suggests that it is indeed rigid and that at least the four secondary amines remain stereochemically active in solution. In this case, it should be possible to separate the two enantiomers that are formed.

The ^{13}C NMR spectrum of the diamagnetic monobridged lanthanum complex La(L')(trif)$_3$ also has seven peaks, suggesting that it also has a C_2 axis on the NMR time scale (there are 13 carbon atoms excluding the triflate carbons, one of which lies on the axis). However, in contrast to the dibridged complex, there is no C_2 axis in the solid state. If this same structure persists in solution, the complex must be fluxional. The C_2 axis in solution must pass through the single methylene bridge, and this is consistent with the observation that one of the NMR peaks (the one farthest downfield), is approximately half the height of the other six.

For Yb(L)(trif)$_3$ the question of what actually exists in solution is rather difficult to answer, but the ^{1}H NMR spectra do provide some insight into the solution structure. In the solid state, the ytterbium complex has no symmetry and is nine-coordinate instead of ten-coordinate. The proton NMR spectrum has more than 18 lines (the peaks labeled broad and very broad appear to be a series of unresolved peaks), and since there are 36 protons, the complex appears to have no symmetry in solution. If this argument is extended to the other lanthanide complexes, it would suggest that the change in coordination number from ten-coordinate to nine-coordinate occurs between praseodymium and europium. In the case of cerium the proton NMR spectrum has 19 lines (one of which may be H$_2$O), and for praseodymium it has 18 lines. Since this number is equal to half the number of protons in these complexes, they are most likely similar to the lanthanum complex and therefore have a C_2 axis in solution. In this case they are most likely ten-coordinate. The europium species has considerably more than 18 lines (at least 31), and is therefore suggested to be nine-coordinate and analogous to the ytterbium analogue. This difference in coordination number for La(L)(trif)$_3$ compared to Eu(L)(trif)$_3$ could account for the differences in reactivity of La(L')(trif)$_3$ compared to Eu(L')(trif)$_3$ toward bis(dimethylamino)methane, since there would presumably be less steric hindrance in the nine-coordinate case. The ^{13}C NMR spectrum of the diamagnetic yttrium species has eight peaks (as compared to seven for lanthanum). Since there are 14 carbons, this suggests that it too is nine-coordinate and analogous to the ytterbium complex. The NMR spectrum of Yb(L'')(trif)$_3$·CH$_3$CN is significantly different from that of Yb(L)(trif)$_3$. There is a large number of peaks spread over a similar range as for Yb(L)(trif)$_3$, and the peak widths are considerably narrower in comparison.

The most exciting feature of the fully encapsulated ytterbium compound, Yb(L'')(trif)$_3$·CH$_3$CN, is its apparent stability toward hydrolysis. Acetonitrile solutions of La(L)(trif)$_3$ and Yb(L)(trif)$_3$ form precipitates immediately upon addition of H$_2$O, whereas this new complex is soluble in H$_2$O and shows no evidence for precipitation. This apparent stability toward hydrolysis suggests that there are no primary amine nitrogens in the ligand structure. The rapid hydrolysis of the doubly bridged compounds may be due to the ability of the primary amines in the ligand to decoordinate from the metal and accept a proton from water, thereby leaving a coordination site open for attack by the newly formed hydroxide ion. A bicyclic ligand in which all of the amines are coordinated secondary amines is not capable of accepting a proton from H$_2$O and therefore is not easily hydrolyzed. These observations are consistent with a lanthanide that has been encapsulated by the amine ligand structure. The compound is soluble in H$_2$O, MeOH, EtOH, and CH$_3$CN.

Electrochemistry. The cyclic voltammograms for Eu(L)$^{3+}$ and Yb(L)$^{3+}$ are illustrated in Figures 2 and 3, respectively. The peak separations at a scan rate of 200 mV/s are 120 and 110 mV for Eu(L)$^{3+}$ and Yb(L)$^{3+}$, respectively. The deviation of these values from that expected for a completely reversible mass-transfer-limited process (peak separation of 59 mV),[1] illustrates the quasi-reversibility of these couples. In both cases the peak separation increases as the scan rate is increased, suggesting that the irreversibility is due to slow electron transfer at the electrode.[17] At a scan rate of 50 mV/s the peak separations are 102 and 94

(17) Bard, A. J.; Faulkner, L. A. *Electrochemical Methods*; Wiley: New York, 1980; Chapters 5 and 6.
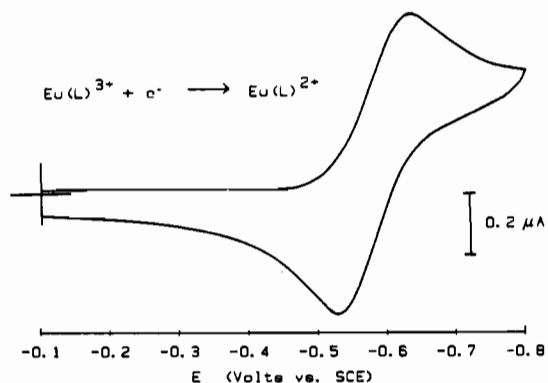
Figure 2. Cyclic voltammogram of 3 mM Eu(L)(trif)$_3$ in propylene carbonate solution with 0.1 M tetraethylammonium perchlorate (scan rate = 200 mV/s).
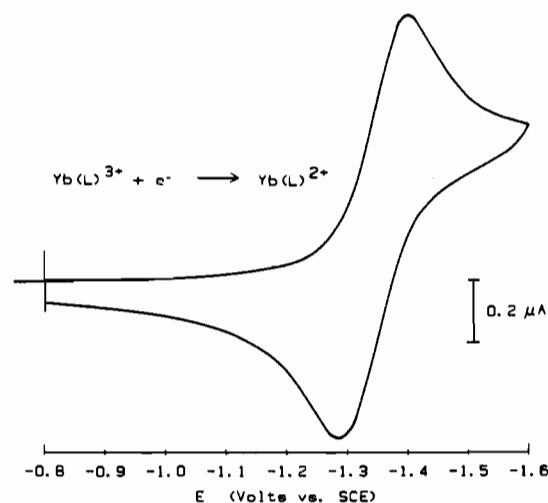

Figure 3. Cyclic voltammogram of 3 mM Yb(L)(trif)$_3$ in propylene carbonate solution with 0.1 M tetraethylammonium perchlorate (scan rate = 200 mV/s).

Figure 4. Plot of potential (E) versus $\log[(i_L - i)/i]$ for Eu(L)(trif)$_3$ obtained from the current versus potential trace of a normal-pulse polarogram performed at a scan rate of 5 mV/s and a pulse amplitude of 50 mV.
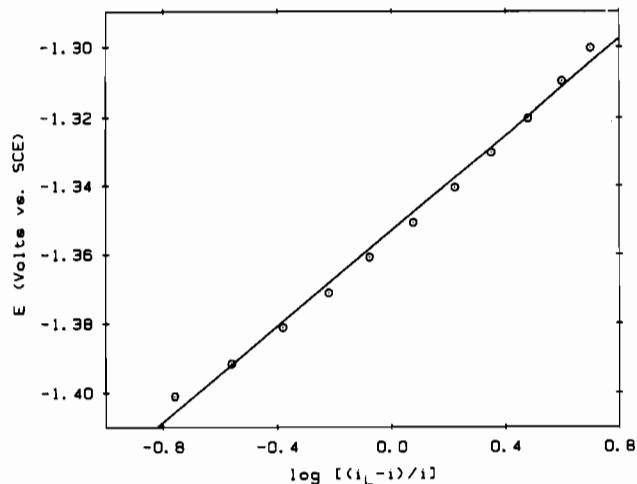

Figure 5. Plot of potential (E) versus $\log[(i_L - i)/i]$ for Yb(L)(trif)$_3$ obtained from the current versus potential trace of a normal-pulse polarogram performed at a scan rate of 5 mV/s and a pulse amplitude of 50 mV.
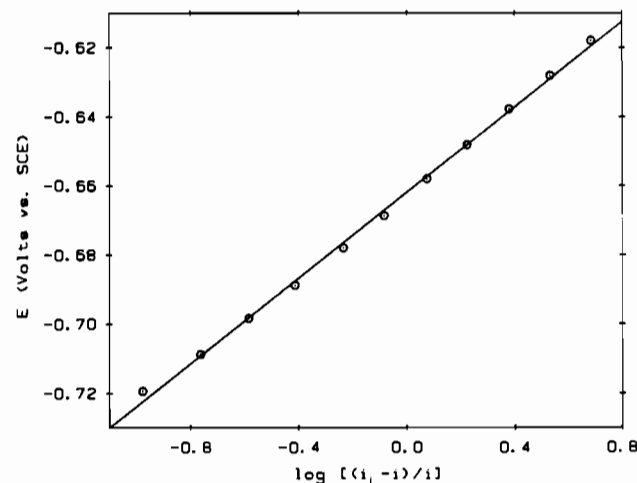
mV for Eu(L)$^{3+}$ and Yb(L)$^{3+}$, respectively, and the ratios of the peak currents are $\simeq 1$. The plots of potential versus $\log[(i_L - i)/i]$ from the corresponding normal-pulse polarograms for Eu(L)$^{3+}$ and Yb(L)$^{3+}$ are illustrated in Figures 4 and 5, respectively. The plot for the europium complex is nearly linear with a slope of 62 mV, indicating that the electrode reaction is a quasi-reversible, Nernstian, one-electron process.[17] The corresponding plot for the ytterbium complex is similar with a slope of 70 mV.

The differential-pulse experiments also provide some information about the degree of reversibility. For a completely reversible one-electron process, the peak width at half-height would be expected to be 95 mV,[17] and in both cases the peak widths at half-height are 110 mV. The formal reduction potentials ($E°'$) obtained from the peak potentials of the differential pulse experiments[17] are −0.68 and −1.37 V (vs SCE, propylene carbonate) for Eu(L)$^{3+}$ and Yb(L)$^{3+}$, respectively.

The measured reduction potentials are directly related to the stabilities, K_{III} and K_{II}, of Ln(III) and Ln(II) with the macrocyclic ligand by the relationship[18]

$$E_c°' - E_s°' = 0.059 \log (K_{II}/K_{III})$$

where $E_c°'$ and $E_s°'$ are the formal reduction potentials of the Ln(III,II) redox couple with and without the ligand, L, in propylene carbonate. Since the formal reduction potentials can be approximately identified with half-wave potentials, by using the half-wave potentials of −0.01 and −0.685 V (vs SCE) for the Eu(III,II) and Yb(III,II) couples, respectively, in the absence of coordinating ligands in propylene carbonate,[19] $\log (K_{III}/K_{II})$ is

calculated to be 11.3 and 11.6, respectively. In order to ascertain the origin of the approximately 680-mV stabilization of the +3 to +2 lanthanide oxidation states by these ligands, the linear triethylenetetramine (trien) was used as a comparison. In trial experiments with trien in CH$_3$CN, the Yb(trien)$_2$$^{3+/2+}$ couple was found to give a shift in potential of 450 mV. Thus about two-thirds of the 680-mV potential shift seen in the Eu and Yb macrocycle complexes can simply be assigned to the greater relative amine complexation of the +3 relative to +2 oxidation state. The remaining one-third of the shift we assign to the macrocyclic effect of these ligands and to the fact that the cavity size is too small to accommodate well the larger +2 ions. The difference in the ionic radius between Yb(III) and Yb(II) is expected to be at least 0.15 Å for nine-coordinate complexes, and for europium the difference is 0.18 Å.[20] The similarity of the stability constant ratios for Eu(L)$^{3+}$/Eu(L)$^{2+}$ and Yb(L)$^{3+}$/Yb(L)$^{2+}$ is consistent with the similarity in these metal ions size differences. Also, the advantages associated with the smaller size of the central metal ion in forming a stable conformation of these macrocycles have been suggested from the single-crystal X-ray structural studies of the La(III) and Yb(III) complexes for the ligand L.[8]

Similar experiments were performed in acetonitrile solution with lithium triflate as the electrolyte. The $E°'$ values determined from

(18) Meites, L. *Polarographic Techniques*, 2nd ed.; Interscience: New York, 1965; Chapter 5.

(19) Massaux, J.; Duyckaerts, G. *Anal. Chim. Acta* **1974**, *73*, 416.
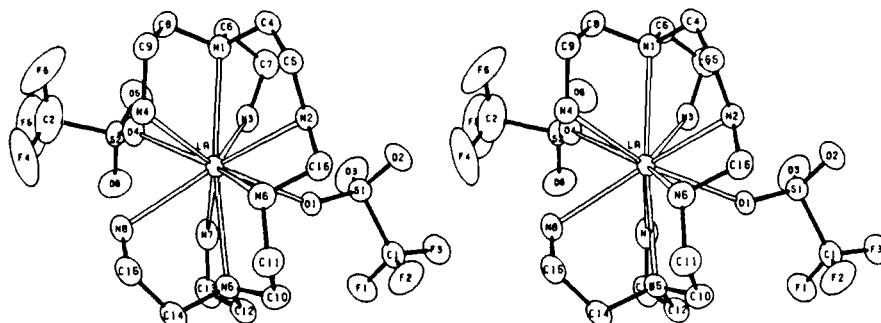(20) Shannon, R. D. *Acta. Crystallogr.* **1976**, *A32*, 751–767.

Figure 6. Stereoview of the labeling diagram for the cation [La(L′)(trif)₂]⁺. This view was chosen to reflect the similarities to the cation [La(L)(trif)₂]⁺.

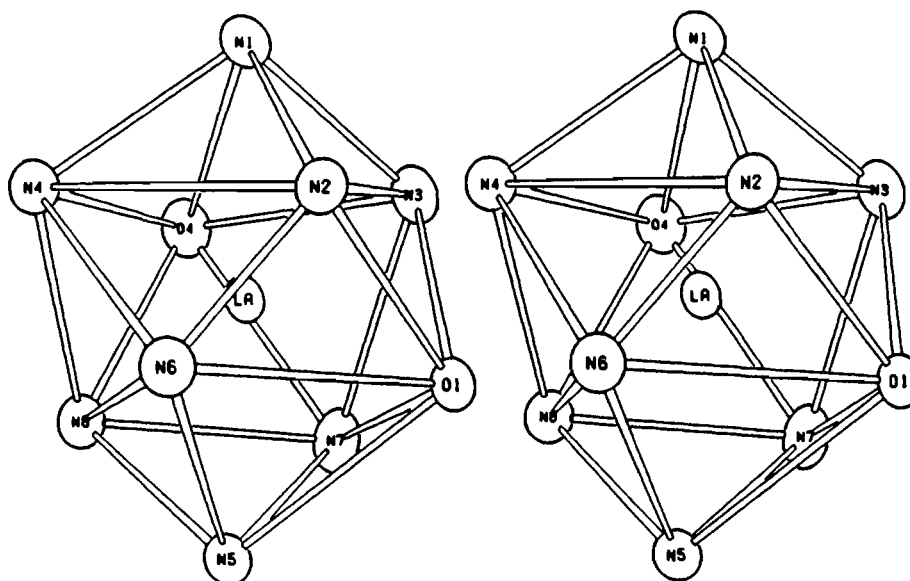**Figure 7.** Stereoview of the coordination geometry for [La(L′)(trif)₂]⁺. The caps of the distorted bicapped square antiprism are N1 and N5, and the two nitrogens connected by the methylene unit, N2 and N6, are facing out. The pseudo-2-fold axis bisects the N2–La–N6 angle.

cyclic voltammetry in acetonitrile are −0.71 and −1.41 V for Eu(L)(trif)₃ and Yb(L)(trif)₃, respectively. A similar degree of quasi-reversibility was observed, with peak separations of 125 and 141 mV for Eu and Yb, respectively, at a scan rate of 200 mV/s. The small shifts in the formal reduction potentials to more negative values in this solvent relative to propylene carbonate suggest that the two solvents have approximately the same relative affinities for the +3 and +2 oxidation states. The relative solvation energies are quite different in propylene carbonate and water, and for the Sm[2.2.2] and Sm[2.2.1] cryptate complexes the potentials in aqueous solution are shifted (in the positive direction) as much as 350 mV relative to those observed in propylene carbonate.[21]

Structure of La(L′)(trif)₃. This structure is similar in many ways to the structure of the corresponding lanthanum complex with two methylene bridges, La(L)(trif)₃·CH₃CN.[8] The stereoview of the cation, [La(L′)(trif)₂]⁺, in Figure 6 was drawn in such a way as to illustrate these similarities.[14,22] Atomic positional and thermal parameters, bond distances and bond angles are listed in Tables III–V, respectively. (Tables of torsion angles (Table S-I), hydrogen bonds (Table S-II), anisotropic thermal parameters (Table S-III), root-mean-square amplitudes of thermal vibration (Table S-IV), calculated hydrogen atom parameters (Table S-V), and F₀ and F_c (Table S-VI) can be found in the supplementary material.[23]) Two of the triflates (S2 and S3) are disordered, and stereoviews of the disorder models are illustrated in Figures S-1 and S-2 in the supplementary material.[23] Stereoviews of the

hydrogen bonding and the unit cell packing diagram are illustrated in Figures S-3 and S-4, respectively.[23] In contrast to the structure of [La(L)(trif)₂]⁺, which has an approximate 2-fold axis, this complex has no symmetry in the solid state.

The coordination geometry illustrated in Figure 7 is similar to that observed in La(L)(trif)₃[7] and can be viewed as a bicapped square antiprism (BSAP). The two tertiary amines, N1 and N5, form the caps, and the two squares are made up of three nitrogens and one triflate oxygen (N2, N3, N4, O4 and N6, N7, N8, O1). This view is rotated around the La–N1 vector relative to Figure 6 so that the two nitrogens closest to the viewer are the ones that are connected with the methylene unit. This view (ignoring atom types and alkyl bridge conformations) illustrates a pseudo-2-fold axis, which bisects N2 and N6 and passes through the lanthanum ion. The dihedral angles are listed in Table VI along with those for [La(L)(trif)₂]⁺ and for an idealized BSAP.

A comparison of the bond lengths and angles in La(L′)(trif)₃ to those seen in the dibridged complex[8] provides useful information about the effects of adding a single methylene bridge. The corresponding values for La(L)(trif)₃ are included in brackets for comparison.[8] The La–N bond lengths (Table IV) range from 2.690 (2) [2.669 (2)] to 2.902 (2) Å [2.816 (2) Å], with an average of 2.759 Å [2.734 Å]. The two tertiary nitrogens (N1 and N5) have La–N distances that are on the average 0.17 Å [0.12 Å] longer than the other La–N distances. The average ethylene-bridged N–N distance is 2.92 Å [2.92 Å], and the single methylene-bridged N–N distance is 2.360 (3) Å [average = 2.36 Å]. The closest nonbridged N–N distances are N3–N7 (3.156 (4) Å) and N4–N8 (3.068 (3) Å) [for the dibridged complex they are N2–N6 (3.29 Å) and N3–N8 (3.27 Å)]. The ethylene-bridged N–La–N angles range from 61.49 (6) [62.50 (10)] to 64.16 (9)° [64.66 (10)°] with an average of 62.8° [63.9°]. The single methylene-bridged angle (N2–La–N6) is 51.02° [average =

(21) Bunzli, J. *Handbook on the Physics and Chemistry of Rare Earths*; Gschneider, K. A., Jr., Eyring, L., Eds.; Elsevier: Amsterdam, 1987; Vol. 9, Table 24.
(22) For purposes of comparison, the cation in this illustration is related by inversion to the one whose positional parameters are given in the tables.
(23) Please see paragraph at end of paper regarding supplementary material.

Table III. Heavy-Atom Positional Parameters and Their Estimated Standard Deviations for La(L′)(trif)$_3$[a]

atom	x	y	z	B, Å^2
La	0.24568 (1)	0.23596 (1)	0.27135 (1)	1.861 (2)
S1	0.29505 (7)	−0.07440 (6)	0.45757 (4)	2.72 (1)
S2	−0.1270 (1)	0.4937 (1)	0.29771 (6)	2.60 (2)
S2′	−0.0857 (2)	0.5576 (2)	0.2942 (1)	2.50 (5)
S2″	−0.108 (1)	0.502 (1)	0.2370 (7)	4.3 (2)*
S3	0.22226 (8)	0.67820 (7)	0.96191 (4)	3.29 (2)
F1	0.1908 (2)	−0.2389 (2)	0.4254 (1)	4.44 (4)
F2	0.4241 (2)	−0.2797 (2)	0.3913 (1)	5.19 (5)
F3	0.3167 (2)	−0.3209 (2)	0.5221 (1)	5.19 (4)
F4	−0.1479 (3)	0.6228 (4)	0.1464 (2)	9.4 (1)
F5	−0.3283 (3)	0.6860 (3)	0.2466 (2)	11.7 (1)
F6	−0.1077 (4)	0.7288 (3)	0.2323 (3)	10.1 (1)
F6′	−0.2314 (8)	0.4557 (7)	0.2356 (5)	5.6 (2)*
F7′	0.331 (2)	0.777 (1)	1.032 (1)	6.0 (3)*
F7	−0.0186 (2)	0.8257 (2)	1.0333 (2)	5.22 (6)
F8	0.1512 (3)	0.7594 (3)	1.1017 (2)	9.70 (8)
F9	0.1584 (3)	0.9120 (2)	0.9873 (3)	10.9 (1)
O1	0.2804 (2)	0.0021 (2)	0.3728 (1)	2.40 (4)
O2	0.4323 (2)	−0.0885 (2)	0.4779 (1)	4.73 (5)
O3	0.1667 (3)	−0.0439 (2)	0.5215 (1)	5.60 (7)
O4	0.0352 (2)	0.4500 (2)	0.2639 (1)	3.25 (5)
O5	−0.1611 (3)	0.5214 (3)	0.3779 (2)	5.42 (7)
O6′	−0.0767 (8)	0.6835 (8)	0.2851 (5)	4.4 (2)*
O6	−0.2129 (3)	0.4193 (3)	0.2863 (4)	4.80 (8)
O7′	0.060 (2)	0.716 (2)	0.948 (1)	5.8 (4)*
O7	0.1842 (3)	0.5665 (2)	1.0137 (2)	4.86 (7)
O8′	0.295 (2)	0.715 (2)	0.882 (1)	5.3 (4)*
O8	0.1762 (4)	0.7312 (4)	0.8848 (2)	7.0 (1)
O9′	0.256 (2)	0.550 (1)	1.0041 (9)	4.4 (3)*
O9	0.3755 (3)	0.6740 (3)	0.9551 (2)	5.84 (9)
N1	0.3135 (2)	0.4064 (2)	0.3458 (1)	2.74 (5)
N2	0.5014 (2)	0.1422 (2)	0.3312 (1)	2.34 (4)
N3	0.0961 (2)	0.2544 (2)	0.4300 (1)	3.04 (5)
N4	0.3554 (2)	0.4340 (2)	0.1645 (1)	2.92 (5)
N5	0.2731 (2)	0.0370 (2)	0.1824 (1)	2.75 (5)
N6	0.5219 (2)	0.1117 (2)	0.1949 (1)	2.66 (5)
N7	0.0081 (2)	0.1480 (2)	0.3021 (2)	3.38 (6)
N8	0.1500 (2)	0.3129 (2)	0.1246 (1)	3.29 (5)
C1	0.3088 (3)	−0.2379 (3)	0.4485 (2)	3.14 (6)
C2	−0.1770 (6)	0.6465 (6)	0.2258 (4)	7.0 (2)
C2′	−0.212 (1)	0.570 (1)	0.2289 (6)	3.3 (2)*
C3	0.1259 (4)	0.8022 (4)	1.0028 (3)	4.6 (1)
C3′	0.207 (3)	0.798 (2)	1.028 (2)	4.9 (5)*
C4	0.4609 (3)	0.3508 (3)	0.3685 (2)	3.05 (6)
C5	0.5660 (3)	0.2502 (3)	0.3191 (2)	2.76 (5)
C6	0.2005 (3)	0.4289 (3)	0.4239 (2)	3.52 (7)
C7	0.1650 (3)	0.3046 (3)	0.4767 (2)	3.54 (7)
C8	0.3069 (3)	0.5348 (3)	0.2851 (2)	3.62 (7)
C9	0.4019 (3)	0.5196 (3)	0.1986 (2)	3.36 (6)
C10	0.4206 (3)	−0.0561 (3)	0.1821 (2)	3.24 (6)
C11	0.5411 (3)	0.0129 (3)	0.1461 (2)	3.42 (7)
C12	0.1611 (3)	−0.0341 (3)	0.2313 (2)	3.46 (7)
C13	0.0102 (3)	0.0554 (3)	0.2528 (2)	4.03 (7)
C14	0.2491 (3)	0.0946 (3)	0.0940 (2)	3.70 (7)
C15	0.2547 (3)	0.2353 (3)	0.0638 (2)	3.84 (7)
C16	0.5810 (3)	0.0554 (3)	0.2725 (2)	2.93 (6)

[a] Starred values are isotropic thermal parameters. The thermal parameter given for anisotropically refined atoms is the isotropic equivalent thermal parameter defined as $(4/3)[a^2B(1,1) + b^2B(2,2) + c^2B(3,3) + ab(\cos \gamma)B(1,2) + ac(\cos \beta)B(1,3) + bc(\cos \alpha)B(2,3)]$, where a, b, and c are real cell parameters and $B(i,j)$ values are anisotropic β's.

51.4°]. The two remaining nonbridged sites have N–La–N angles of 68.80 (7) (N4–La–N8) and 71.76 (9)° (N3–La–N7) [75.84 (10)°]. The angle between the two tertiary nitrogen La–N vectors is 162.67 (6)° [162.35 (9)°]. The nitrogen hydrogens are weakly hydrogen bonded to triflate oxygens both in the same molecule and from neighboring triflate anions (see Figure S-3 and Table S-II in the supplementary material[23]), similar to the H-bonding seen in the dibridged complex.[7]

The ligand conformations in the mono- and dibridged species are strikingly similar despite the fact that La(L′) has one less methylene bridge. The absence of the methylene unit in La(L′) removes the approximate 2-fold axis seen in La(L), since in that

Table IV. Intramolecular Distances (Å) for La(L′)(trif)$_3$

La–O1	2.637 (2)	F3–C1	1.321 (3)
La–O4	2.574 (2)	F4–C2	1.370 (10)
La–N1	2.870 (2)	F4–C2′	1.402 (11)
La–N2	2.743 (2)	F5–C2	1.375 (7)
La–N3	2.695 (2)	F5–C2′	1.446 (11)
La–N4	2.728 (2)	F6–C2	1.348 (14)
La–N5	2.902 (2)	F6′–C2′	1.306 (14)
La–N6	2.738 (2)	F7–C3	1.327 (7)
La–N7	2.690 (2)	F7′–C3′	1.18 (3)
La–N8	2.703 (2)	F8–C3	1.343 (6)
		F8–C3′	1.22 (3)
S1–O1	1.457 (2)	F9–C3	1.293 (6)
S1–O2	1.434 (2)	F9–C3′	1.25 (3)
S1–O3	1.425 (2)		
S1–C1	1.816 (3)	N1–C4	1.488 (3)
S2–O4	1.496 (2)	N1–C6	1.487 (4)
S2–O5	1.394 (4)	N1–C8	1.488 (4)
S2–O6	1.441 (5)	N2–C5	1.472 (3)
S2–C2	1.784 (8)	N2–C16	1.456 (3)
S2′–O4	1.468 (3)	N3–C7	1.479 (4)
S2′–O5	1.410 (4)	N4–C9	1.477 (4)
S2′–O6′	1.387 (12)	N5–C10	1.474 (4)
S2′–C2′	1.834 (11)	N5–C12	1.487 (4)
S2″–O4	1.483 (11)	N5–C14	1.496 (3)
S2″–O6	1.518 (12)	N6–C11	1.481 (4)
S3–O7′	1.581 (20)	N6–C16	1.470 (3)
S3–O7	1.393 (2)	N7–C13	1.484 (4)
S3–O8′	1.350 (18)	N8–C15	1.472 (4)
S3–O8	1.399 (3)		
S3–O9′	1.367 (20)	C4–C5	1.509 (4)
S3–O9	1.466 (3)	C6–C7	1.501 (4)
S3–C3	1.795 (5)	C8–C9	1.516 (4)
S3–C3′	1.91 (3)	C10–C11	1.514 (4)
		C12–C13	1.497 (5)
F1–C1	1.329 (3)	C14–C15	1.508 (4)
F2–C1	1.311 (4)		

case the two methylene bridges were related by the 2-fold axis. However, the pseudo-2-fold axis seen in Figure 7 passes through the methylene unit, and as suggested above, the time-averaged solution structure does indeed have a C_2 axis. The fluxional process must involve coordination and decoordination of the triflate anions, since the two that are coordinated in the structure are not related by symmetry.

At this point it is appropriate to speculate about the possible explanations for the difficulty of obtaining the fully encapsulated lanthanide ion. The most remarkable difference between the mono-bridged and dibridged complexes is between the closest nonbridged N–N distances. Both of these distances for the mononobridged complex are shorter than the corresponding distance in the dibridged complex, and therefore the effect of adding a methylene bridge is to pull the closest nonbridged distances apart. Apparently, the gap for the dibridged complex is too large for a methylene bridge.

Another possibility that has already been mentioned is the fact that the triflate anions may be coordinated in solution and sterically blocking the site of attack. One method of determining whether or not the triflates are coordinated in solution is conductivity, which can determine the overall charge on the complex. The conductivities listed in Table VII are compared to those of 1:1, 1:2, and 1:3 electrolytes.[24] These values are very dependent on concentration, which indicates that acetonitrile competes effectively with the triflate anions for the empty coordination sites. At millimolar concentrations the dibridged and monobridged lanthanum complexes appear to be 1:1 and 2:1 electrolytes, respectively. This may be an indication of stronger anion binding in the dibridged complex and could partially account for the lower reactivity of this species toward the coupling reagent. The values for the europium and ytterbium complexes suggest 2:1 electrolytes at this concentration.

Another hindering force may be the hydrogen bonding of the amines to the triflate oxygens, in particular the intramolecular

(24) Geary, W. J. *Coord. Chem. Rev.* **1971**, *7*, 81–122.

Table V. Intramolecular Angles (deg) for La(L′)(trif)$_3$

O1–La–O4	134.48 (6)	O8–S3–C3	104.12 (23)
O1–La–N1	108.73 (6)	O8′–S3–C3′	109.3 (12)
O1–La–N	265.15 (5)	O9′–S3–C3′	113.2 (13)
O1–La–N3	69.29 (7)	O9–S3–C3	101.0 (3)
O1–La–N4	151.44 (6)	La–O1–S1	146.42 (10)
O1–La–N5	68.87 (5)	La–O4–S2	138.42 (16)
O1–La–N6	80.07 (6)	La–O4–S2′	158.11 (15)
O1–La–N7	68.67 (6)	La–O4–S2″	137.7 (5)
O1–La–N8	127.09 (6)	La–N1–C4	112.48 (15)
O4–La–N1	72.90 (6)	La–N1–C6	108.90 (16)
O4–La–N2	135.76 (6)	La–N1–C8	108.67 (15)
O4–La–N3	71.62 (6)	C4–N1–C6	108.52 (20)
O4–La–N4	71.47 (6)	C4–N1–C8	109.80 (21)
O4–La–N5	121.65 (6)	C6–N1–C8	108.38 (21)
O4–La–N6	145.40 (6)	La–N2–C5	109.93 (14)
O4–La–N7	77.73 (7)	La–N2–C16	96.21 (13)
O4–La–N8	66.95 (7)	C5–N2–C16	113.12 (19)
N1–La–N2	62.86 (6)	La–N3–C7	114.37 (18)
N1–La–N3	64.16 (9)	La–N4–C9	120.18 (16)
N1–La–N4	62.49 (6)	La–N5–C10	108.28 (14)
N1–La–N5	162.67 (6)	La–N5–C12	107.29 (16)
N1–La–N6	100.70 (6)	La–N5–C14	112.28 (16)
N1–La–N7	132.64 (7)	C10–N5–C12	108.64 (21)
N1–La–N8	124.12 (7)	C10–N5–C14	110.52 (22)
N2–La–N3	88.43 (7)	C12–N5–C14	109.71 (20)
N2–La–N4	87.80 (6)	La–N6–C11	119.99 (15)
N2–La–N5	102.05 (6)	La–N6–C16	96.09 (14)
N2–La–N6	51.02 (6)	C11–N6–C16	113.32 (21)
N2–La–N7	133.66 (6)	La–N7–C13	119.03 (17)
N2–La–N8	140.88 (7)	La–N8–C15	109.16 (16)
N3–La–N4	121.49 (8)		
N3–La–N5	126.93 (8)	S1–C1–F1	110.78 (20)
N3–La–N6	137.27 (7)	S1–C1–F2	111.28 (19)
N3–La–N7	71.76 (9)	S1–C1–F3	110.43 (21)
N3–La–N8	130.35 (7)	F1–C1–F2	107.30 (24)
N4–La–N5	110.89 (6)	F1–C1–F3	107.37 (22)
N4–La–N6	75.50 (6)	F2–C1–F3	109.56 (24)
N4–La–N7	138.37 (7)	S2–C2–F4	108.5 (6)
N4–La–N8	68.80 (7)	S2–C2–F5	104.5 (6)
N5–La–N6	62.02 (6)	S2–C2–F6	109.3 (6)
N5–La–N7	63.57 (7)	S2″–C2–F5	115.9 (9)
N5–La–N8	61.49 (6)	S2″–C2–F6	122.2 (7)
N6–La–N7	123.88 (7)	F4–C2–F5	103.6 (6)
N6–La–N8	91.81 (7)	F4–C2–F6	114.4 (7)
N7–La–N8	73.75 (7)	F5–C2–F6	115.8 (8)
		S2′–C2′–F4	104.8 (7)
O1–S1–O2	113.64 (11)	S2′–C2′–F5	101.7 (6)
O1–S1–O3	114.41 (13)	S2′–C2′–F6′	111.3 (8)
O1–S1–C1	102.12 (11)	F4–C2′–F5	98.5 (7)
O2–S1–O3	116.19 (16)	F4–C2′–F6′	112.7 (9)
O2–S1–C1	103.83 (13)	S3–C3–F7	110.7 (4)
O3–S1–C1	104.41 (14)	S3–C3–F8	110.4 (3)
O4–S2–O5	112.95 (22)	S3–C3–F9	112.4 (4)
O4–S2–O6	115.67 (24)	F7–C3–F8	104.3 (4)
O4–S2–C2	101.0 (3)	F7–C3–F9	107.7 (4)
O4–S2–C2′	112.6 (4)	F8–C3–F9	111.0 (5)
O5–S2–O6	115.3 (3)	S3–C3′–F7′	101.7 (19)
O5–S2–C2	106.9 (4)	S3–C3′–F8	109.4 (19)
O5–S2–C2′	124.5 (4)	S3–C3′–F9	107.4 (19)
O6–S2–C2	103.0 (4)	F7′–C3′–F8	102.0 (24)
O4–S2′–O5	113.8 (3)	F7′–C3′–F9	112.0 (24)
O4–S2′–O6′	125.1 (5)	F8–C3′–F9	122.4 (23)
O4–S2′–C2′	97.9 (4)	N1–C4–C5	114.00 (21)
O5–S2′–O6′	106.4 (5)	N2–C5–C4	109.80 (20)
O5–S2′–C2′	104.2 (5)	N1–C6–C7	112.11 (22)
O6′–S2′–C2′	107.0 (5)	N3–C7–C6	109.75 (23)
O4–S2″–O6	111.9 (8)	N1–C8–C9	112.31 (23)
O4–S2″–C2	117.0 (8)	N4–C9–C8	109.73 (23)
O6–S2″–C2	114.5 (8)	N5–C10–C11	111.84 (22)
O7′–S3–O8′	101.1 (13)	N6–C11–C10	110.67 (22)
O7′–S3–O9′	107.5 (17)	N5–C12–C13	113.24 (23)
O7′–S3–C3′	102.4 (12)	N7–C13–C12	111.79 (22)
O7–S3–O8	119.05 (23)	N5–C14–C15	113.08 (22)
O7–S3–O9	113.44 (24)	N8–C15–C14	109.24 (24)
O7–S3–C3	103.6 (3)	N2–C16–N6	107.56 (19)
O8–S3–O9	112.88 (22)		

hydrogen bonding. This could hinder the reactivity in one of two ways. If the mechanism involves deprotonation of the amine before

Table VI. Polyhedral Angles (deg) for [La(L)(trif)$_2$]$^+$ and [La(L′)(trif)$_2$]$^+$

	La(L)		La(L′)		angle idealized for BSAP^a
edge	angle	av angle	angle	av angle	
a	46.7	46.7	72.1	72.1	56.2
b	60.9		70.3		56.3
b′	62.2	61.6	71.6	71.0	
c	28.3		12.2		30.9
c′	23.5	25.9	16.9	14.6	
d	45.8		17.5		30.9
d′	44.2	45.0	13.7	15.6	
e	54.0		58.1		56.2
e′	57.2	55.6	55.5	56.8	
f	50.8		61.7		56.2
f′	53.4	52.1	54.1	57.9	
g	45.6		66.4		56.3
g′	47.7	46.7	65.0	65.7	
h	64.1		66.0		56.3
h′	65.4	64.8	50.1	58.1	
i	26.2		41.6		30.9
i′	26.7	26.5	38.8	40.2	
j	66.9		42.2		56.3
j′	66.1	66.5	54.4	48.3	
k	70.8		52.2		56.2
k′	69.5	70.2	52.5	52.4	
l	53.1	53.1	41.1	41.1	56.2
m	15.3		38.3		30.9
m′	14.5	14.9	45.2	41.8	

^{a} See reference 28.

attack, then the hydrogen bonding would make the hydrogens more difficult to remove. If the mechanism involves decoordination of the primary amine before it attacks, then the intramolecular hydrogen bonding may actually prevent the amine from decoordinating. Albeit there is no evidence for the hydrogen bonding in solution, a change in the solvent to a more polar protic solvent such as methanol may clarify this.

Another very real possibility, and probably the most likely one, is that the lanthanum ion is simply too large for the proposed cage structure. There is some support for this in the electrochemical results, as described earlier. Additional evidence for this lies in the fact that the fully encapsulated complex was prepared by using a significantly smaller lanthanide, ytterbium. However, even in the case of ytterbium it appears to be very difficult to prepare such a complex. It may well be possible to prepare the scandium complex; this is currently under investigation.

Structure of Pr(tren)(trien)(trif)$_3$. Figure 8 illustrates the structure and labeling scheme, and Figure 9 illustrates a stereoview of the [Pr(tren)(trien)(trif)]$^{2+}$ cation. The complex is nine-coordinate with eight amine donors and one oxygen donor from a coordinating triflate anion. Atomic positional and thermal parameters,[25] bond distances, and bond angles are listed in Tables VIII–X, respectively. (Tables of torsion angles (Table S-VII), hydrogen bonds (Table S-VIII), anisotropic thermal parameters (Table S-IX), root-mean-square amplitudes of thermal vibration (Table S-X), calculated hydrogen atom parameters (Table S-XI), and F_o and F_c (Table S-XII) can be found in the supplementary material.[23]) The coordinated triflate anion is disordered.[26] The coordination geometry is illustrated in Figure 10 and is best described as a monocapped, square antiprism. The dihedral angles are listed in Table XI. The tertiary amine of tren (N1, the

(25) The high thermal parameters in the triflate anions are probably due to unresolved disorder.

(26) The disorder in the coordinated triflate was modeled by including a partial occupancy fluorine, F23, between F2 and F3. The occupancy of F23 was assigned a value of 0.5, and the occupancies of F2 and F3 were reduced accordingly.

Table VII. Conductivities of Lanthanide Amine Complexes in Acetonitrile

compd	concn, mM	conductivity, cm^2 Ω^{-1} mol^{-1}
La(L)(trif)$_3$	0.96	150
La(L′)(trif)$_3$	0.97	260
Pr(L)(trif)$_3$	1.2, 0.58	190, 230
Eu(L)(trif)$_3$	1.0, 0.52	230, 270
Yb(L)(trif)$_3$	1.3, 0.63	220, 260
1:1 electrolyte	1.0	120–160
2:1 electrolyte	1.0	220–300
3:1 electrolyte	1.0	340–420
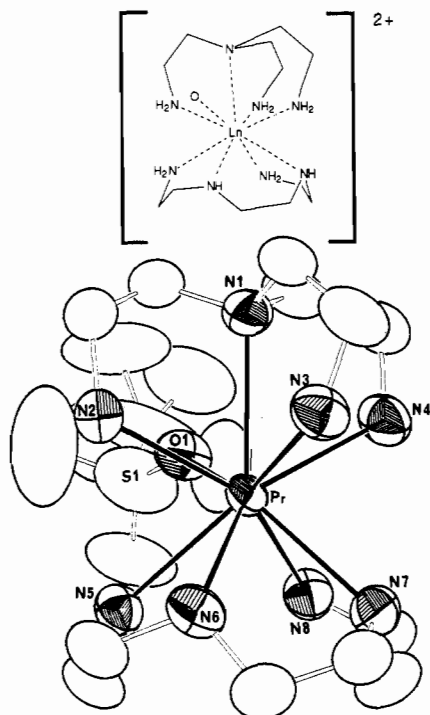
Figure 8. Labeling diagram for the cation [Pr(tren)(trien)(trif)]$^{2+}$ along with a schematic drawing of the complex. The triflate anion is disordered.

capping atom), its three primary amines (N2, N3, N4), and the triflate oxygen generate the upper square, and the four nitrogens from trien (N5, N6, N7, N8) make up the lower square.

The bond lengths and angles in this complex provide some information concerning appropriate encapsulation bridge lengths, as well as typical values for these particular ligands. The Pr–N bond lengths range from 2.634 (7) to 2.737 (7) Å with an average

Table VIII. Heavy-Atom Positional Parameters and Their Estimated Standard Deviations for Pr(tren)(trif)$_3$[a]

atom	x	y	z	B, Å^2
Pr	0.17262 (5)	0.31542 (5)	0.24432 (3)	3.279 (9)
S1	−0.1307 (4)	0.5581 (3)	0.2435 (3)	11.0 (1)
S2	0.2784 (3)	0.7449 (2)	0.9329 (1)	4.94 (6)
S3	0.2840 (3)	0.8548 (3)	0.4653 (2)	5.42 (7)
F1	−0.270 (1)	0.7626 (8)	0.2358 (7)	16.6 (4)
F2	−0.066 (2)	0.720 (2)	0.1403 (9)	18.2 (6)
F3	−0.101 (2)	0.722 (1)	0.3096 (7)	20.5 (5)
F4	0.360 (1)	0.9517 (7)	0.9578 (6)	18.3 (3)
F5	0.143 (1)	0.9538 (8)	0.9479 (7)	16.2 (4)
F6	0.204 (1)	0.851 (1)	1.0509 (6)	18.7 (4)
F7	0.5559 (8)	0.8765 (9)	0.4572 (5)	12.3 (3)
F8	0.5041 (9)	0.7043 (7)	0.4350 (5)	10.9 (2)
F9	0.4990 (9)	0.8823 (9)	0.3419 (5)	12.8 (3)
F23	−0.047 (2)	0.778 (1)	0.215 (1)	14.6 (7)
O1	0.0083 (7)	0.5064 (6)	0.2482 (4)	5.9 (2)
O2	−0.2135 (9)	0.5175 (9)	0.1964 (6)	12.5 (3)
O3	−0.227 (2)	0.533 (2)	0.3414 (8)	19.6 (6)
O4	0.391 (1)	0.6759 (8)	0.9653 (6)	10.9 (3)
O5	0.150 (1)	0.6957 (9)	0.9438 (8)	15.4 (4)
O6	0.339 (1)	0.798 (1)	0.8490 (5)	11.9 (3)
O7	0.2666 (8)	0.9940 (6)	0.4452 (4)	6.6 (2)
O8	0.2106 (9)	0.7945 (8)	0.4211 (5)	9.2 (2)
O9	0.2680 (9)	0.7961 (8)	0.5525 (4)	8.5 (2)
N1	0.2869 (8)	0.4566 (7)	0.3261 (4)	4.9 (2)
N2	0.0719 (9)	0.2618 (8)	0.4069 (4)	5.8 (2)
N3	0.4093 (8)	0.2169 (7)	0.2945 (4)	5.0 (2)
N4	0.3662 (9)	0.4943 (8)	0.1485 (5)	5.7 (2)
N5	−0.0972 (8)	0.2324 (7)	0.2685 (4)	4.6 (2)
N6	0.1364 (8)	0.0567 (8)	0.2882 (4)	4.8 (2)
N7	0.3096 (8)	0.1909 (7)	0.1305 (4)	4.8 (2)
N8	0.1088 (8)	0.4019 (7)	0.0942 (4)	5.2 (2)
C1	−0.145 (2)	0.706 (1)	0.228 (1)	24.2 (6)
C2	0.251 (2)	0.887 (1)	0.9682 (8)	9.5 (4)
C3	0.471 (1)	0.828 (1)	0.4238 (7)	7.3 (3)
C4	0.176 (1)	0.4682 (9)	0.3997 (6)	6.5 (3)
C5	0.120 (1)	0.340 (1)	0.4553 (6)	6.5 (3)
C6	0.420 (1)	0.398 (1)	0.3537 (6)	5.9 (3)
C7	0.500 (1)	0.308 (1)	0.3075 (7)	7.1 (3)
C8	0.315 (1)	0.5880 (9)	0.2690 (6)	6.4 (3)
C9	0.412 (1)	0.587 (1)	0.1878 (6)	6.5 (3)
C10	−0.119 (1)	0.0933 (9)	0.2827 (6)	5.9 (3)
C11	−0.018 (1)	0.0179 (9)	0.3325 (6)	5.9 (3)
C12	0.189 (1)	−0.0091 (9)	0.2219 (6)	6.0 (3)
C13	0.325 (1)	0.0470 (8)	0.1681 (6)	5.7 (3)
C14	0.243 (1)	0.215 (1)	0.0578 (6)	6.9 (3)
C15	0.212 (1)	0.357 (1)	0.0282 (5)	6.2 (3)

[a] The thermal parameter given for anisotropically refined atoms is the isotropic equivalent thermal parameter defined as $(4/3)[a^2B(1,1) + b^2B(2,2) + c^2B(3,3) + ab(\cos\gamma)B(1,2) + ac(\cos\beta)B(1,3) + bc(\cos\alpha)B(2,3)]$, where a, b, and c are real cell parameters and $B(i,j)$ values are anisotropic β's.
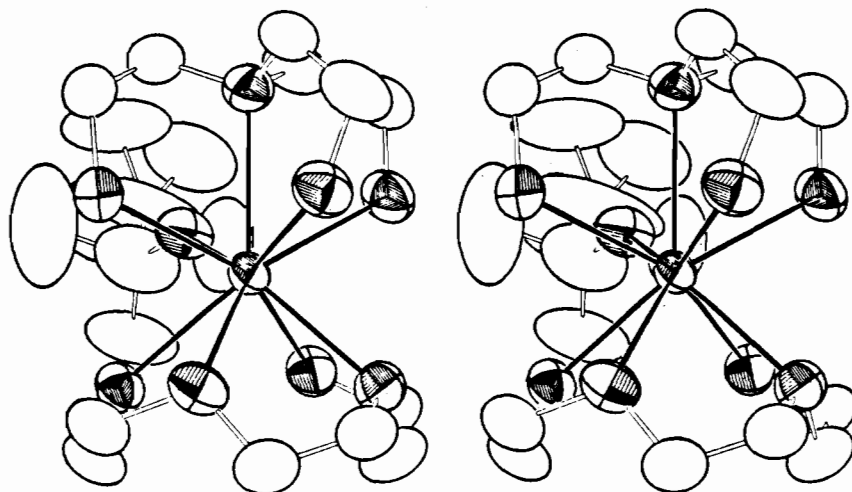
Figure 9. Stereoview of the cation [Pr(tren)(trien)(trif)]$^{2+}$. The coordinating atoms and the praseodymium are shaded, and the four primary amines that would be mostly likely to participate in a bridging reaction (N2, N4, N5, and N8) are in the back of the diagram.
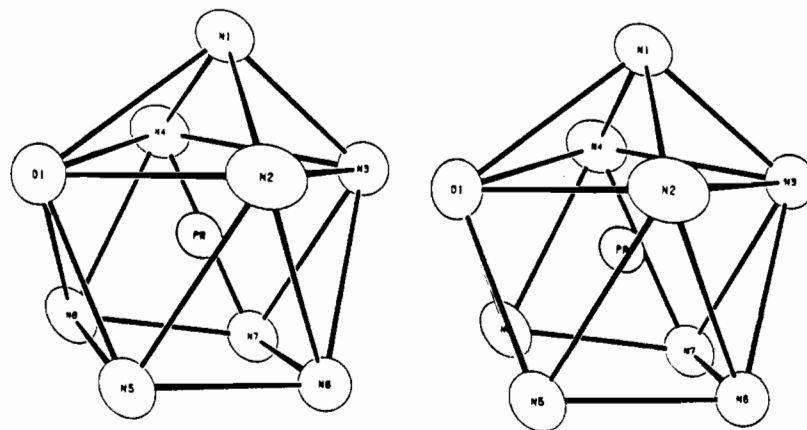
Figure 10. Stereoview of the coordination geometry for the cation $[Pr(tren)(trien)(trif)]^{2+}$. The cap of the distorted monocapped square antiprism is the tertiary amine of tren, N1, and the four nitrogens of trien, N5–N6–N7–N8, make up the lower square.

Table IX. Intramolecular Distances (Å) for Pr(tren)(trien)(trif)$_3$

Pr–O1	2.475 (6)	F4–C2	1.236 (16)
Pr–N1	2.737 (7)	F5–C2	1.262 (19)
Pr–N2	2.642 (7)	F6–C2	1.338 (17)
Pr–N3	2.634 (7)	F7–C3	1.299 (14)
Pr–N4	2.685 (7)	F8–C3	1.303 (13)
Pr–N5	2.690 (7)	F9–C3	1.334 (12)
Pr–N6	2.683 (6)	N1–C4	1.475 (12)
Pr–N7	2.687 (6)	N1–C6	1.484 (11)
Pr–N8	2.670 (6)	N1–C8	1.479 (11)
S1–O1	1.404 (7)	N2–C5	1.480 (12)
S1–O2	1.409 (9)	N3–C7	1.441 (12)
S1–O3	1.675 (13)	N4–C9	1.476 (12)
S1–C1	1.52 (3)	N5–C10	1.461 (11)
S2–O4	1.385 (8)	N6–C11	1.524 (12)
S2–O5	1.324 (9)	N6–C12	1.465 (11)
S2–O6	1.397 (9)	N7–C13	1.503 (11)
S2–C2	1.759 (14)	N7–C14	1.472 (11)
S3–O7	1.435 (6)	N8–C15	1.474 (12)
S3–O8	1.430 (8)	C4–C5	1.494 (14)
S3–O9	1.428 (7)	C6–C7	1.465 (14)
S3–C3	1.792 (11)	C8–C9	1.483 (14)
F1–C1	1.295 (19)	C10–C11	1.479 (13)
F2–C1	1.49 (4)	C12–C13	1.471 (14)
F3–C1	1.59 (4)	C14–C15	1.492 (13)

Table X. Intramolecular Angles (deg) for Pr(tren)(trien)(trif)$_3$

O1–Pr–N1	74.95 (20)	O9–S3–C3	103.6 (5)
O1–Pr–N2	81.55 (23)	Pr–O1–S1	146.1 (4)
O1–Pr–N3	139.27 (20)	Pr–N1–C4	107.4 (5)
O1–Pr–N4	84.05 (24)	Pr–N1–C6	114.1 (5)
O1–Pr–N5	72.74 (20)	Pr–N1–C8	106.8 (5)
O1–Pr–N6	134.42 (22)	C4–N1–C6	109.0 (7)
O1–Pr–N7	137.31 (21)	C4–N1–C8	108.7 (8)
O1–Pr–N8	72.81 (21)	C6–N1–C8	110.7 (7)
N1–Pr–N2	64.50 (22)	Pr–N2–C5	119.1 (6)
N1–Pr–N3	64.33 (20)	Pr–N3–C7	116.0 (5)
N1–Pr–N4	64.12 (22)	Pr–N4–C9	117.5 (6)
N1–Pr–N5	130.77 (20)	Pr–N5–C10	118.6 (5)
N1–Pr–N6	126.99 (20)	Pr–N6–C11	112.9 (5)
N1–Pr–N7	128.86 (21)	Pr–N6–C12	115.7 (5)
N1–Pr–N8	126.73 (22)	C11–N6–C12	110.7 (7)
N2–Pr–N3	80.88 (24)	Pr–N7–C13	111.9 (5)
N2–Pr–N4	128.60 (23)	Pr–N7–C14	113.2 (5)
N2–Pr–N5	74.78 (22)	C13–N7–C14	110.5 (7)
N2–Pr–N6	76.61 (22)	Pr–N8–C15	113.7 (5)
N2–Pr–N7	138.36 (22)	S1–C1–F1	120.7 (22)
N2–Pr–N8	145.90 (25)	S1–C1–F2	89.3 (14)
N3–Pr–N4	78.85 (23)	S1–C1–F3	100.0 (27)
N3–Pr–N5	135.65 (21)	S1–C1–F23	125.6 (18)
N3–Pr–N6	75.54 (21)	F1–C1–F2	113.9 (32)
N3–Pr–N7	74.96 (21)	F1–C1–F3	99.6 (22)
N3–Pr–N8	133.10 (22)	F1–C1–F23	113.6 (21)
N4–Pr–N5	144.56 (22)	F2–C1–F3	134.2 (24)
N4–Pr–N6	140.06 (24)	F2–C1–F23	72.6 (33)
N4–Pr–N7	79.24 (23)	F3–C1–F23	65.6 (20)
N4–Pr–N8	71.31 (22)	S2–C2–F4	116.4 (11)
N5–Pr–N6	63.15 (20)	S2–C2–F5	112.5 (13)
N5–Pr–N7	99.85 (21)	S2–C2–F6	107.5 (12)
N5–Pr–N8	76.35 (21)	F4–C2–F5	114.5 (16)
N6–Pr–N7	64.87 (22)	F4–C2–F6	104.1 (16)
N6–Pr–N8	105.80 (21)	F5–C2–F6	99.7 (12)
N7–Pr–N8	64.67 (22)	S3–C3–F7	112.7 (9)
O1–S1–O2	121.2 (5)	S3–C3–F8	112.1 (9)
O1–S1–O3	107.1 (7)	S3–C3–F9	108.7 (8)
O1–S1–C1	114.9 (9)	F7–C3–F8	106.8 (10)
O2–S1–O3	108.1 (9)	F7–C3–F9	109.0 (12)
O2–S1–C1	109.1 (12)	F8–C3–F9	107.4 (11)
O3–S1–C1	92.2 (17)	N1–C4–C5	113.7 (8)
O4–S2–O5	123.8 (7)	N2–C5–C4	110.6 (8)
O4–S2–O6	104.4 (7)	N1–C6–C7	115.3 (8)
O4–S2–C2	106.6 (8)	N3–C7–C6	113.3 (9)
O5–S2–O6	112.1 (8)	N1–C8–C9	113.5 (8)
O5–S2–C2	107.2 (7)	N4–C9–C8	112.5 (8)
O6–S2–C2	99.9 (7)	N5–C10–C11	109.3 (7)
O7–S3–O8	113.3 (4)	N6–C11–C10	109.7 (8)
O7–S3–O9	113.3 (4)	N6–C12–C13	111.1 (7)
O7–S3–C3	104.3 (5)	N7–C13–C12	111.9 (7)
O8–S3–O9	116.6 (5)	N7–C14–C15	109.6 (8)

of 2.68 Å. The average Pr–N bond length in the 12-coordinate, hexakis(naphthyridine)[27] complex is 2.748 Å. The tertiary amine Pr–N distance of 2.737 (7) Å is significantly longer than the average of the other seven Pr–N bonds of 2.67 Å. The average of the three primary amine Pr–N bonds of tren is 2.65 Å compared to 2.68 Å for the average of the four trien Pr–N bonds. The average of all ethylene-bridged N–N distances is 2.86, that for tren is 2.87, and that for trien is 2.85. The average of all ethylene-bridged N–Pr–N angles is 64.3°, the average of the three in tren is 64.3°, and the average of the three in trien is 64.2°. The closest nonbridged N–N distances are 3.12 Å for N4–N8, 3.24 Å for N2–N5, 3.24 Å for N3–N7, and 3.26 Å for N3–N6. These same pairs of nitrogens have correspondingly the smallest N–Pr–N angles, which are 71.3 (2) [N4–Pr–N8], 74.8 (2) [N2–Pr–N5], 75.0 (2) [N3–Pr–N7], and 75.5 (2)° [N3–Pr–N6]. The nitrogen hydrogens are involved in a weak hydrogen bonding network to the triflate oxygens and these interactions are listed in Table S-VIII and illustrated in Figure S-5 in the supplementary material.[23] A stereoview of the unit cell packing diagram is illustrated in Figure S-6 (also in the supplementary material[23]).

Conclusion

The partial encapsulation described previously has been extended to include selected lanthanide ions, and the synthesis of the mono- and tribridged analogues completes the series. The change in coordination number and ligand conformation observed in the dibridged complexes occurs between praseodymium and europium. These partially closed cage structures impart a large

(27) Clearfield, A.; Gopal, R.; Olsen, R. W. *Inorg. Chem.* **1977**, *16*, 911.
(28) Robertson, B. E. *Inorg. Chem.* **1977**, *16*, 2735.
(29) Guggenberger, L. J.; Muetterties, E. L. *J. Am. Chem. Soc.* **1976**, *98*, 7221.

Table XI. Measured and Idealized Polyhedral Angles (deg) for [La(en)$_4$(trif)]$^{2+}$, [Yb(L)(trif)]$^{2+}$, and [Pr(tren)(trien)(trif)]$^{2+}$

face 1	face 2	angle	av angle	idealized angle
[La(en)$_4$(trif)]$^{2+}$; D_{3h}				
N5,N6,O1	N2,N4,N8	172.7	172.7	180.0
N1,N2,N5	N3,N6,N8	141.1		146.4
N2,N5,N7	N3,N4,O1	146.1	144.8	146.4
N6,N7,N8	N1,N4,O1	147.3		146.4
N1,N2,N5	N2,N5,N7	21.0		26.4
N6,N7,N8	N3,N6,N8	23.9	25.1	26.4
N3,N4,O1	N1,N4,O1	30.4		26.4
[Yb(L)(trif)]$^{2+}$; C_{4v}				
N1,N2,N3	N5,N8,O1	161.4	162.2	163.5
N2,N6,O1	N1,N7,N8	162.9		163.5
N1,N3,N7	N5,N6,O1	147.8	142.6	138.2
N2,N3,N6	N5,N7,N8	137.3		138.2
N3,N5,N6	N3,N5,N7	0.6	0.55	0.0
N3,N6,N7	N5,N6,N7	0.5		0.0
[Pr(tren)(trien)(trif)]$^{2+}$; C_{4v}				
N2,N3,N6	N4,N8,O1	160.4	163.1	163.5
N2,N5,O1	N3,N4,N7	165.7		163.5
N2,N5,N6	N4,N7,N8	145.8	141.9	138.2
N5,N8,O1	N3,N6,N7	138.0		138.2
N5,N6,N7	N5,N7,N8	6.1	6.2	0.0
N6,N7,N8	N5,N6,N8	6.3		0.0

^{a} See reference 29.

stabilization to the +3 oxidation states of europium and ytterbium compared to the +2 states. A comparison of the structures of the mono- and dibridged lanthanum complexes implicate the large size of the metal ion as a possible explanation for the difficulty of obtaining and encapsulated complex. However, it is indeed possible to prepare a ytterbium amine complex that is completely

encapsulated, and the size of the proposed cage structure is apparently appropriate only for the smallest of the lanthanide ions. Finally, the first example of a mixed amine lanthanide complex has been structurally characterized, but it apparently reacts much slower with the formaldehyde coupling reagent than the bis(tren) complexes do.

Contribution from the Department of Chemistry,
University of Houston, University Park, Houston, Texas 77004

cis- and *trans*-Dioxo Complexes of Chlororuthenium(VI)

S. Perrier and J. K. Kochi*

Dioxoruthenium(VI) complexes are prepared as the chloro derivatives O$_2$RuCl$_4$$^{2-}$ and O$_2$RuCl$_3$$^-$ and isolated as the crystalline phosphonium and ammonium salts. Quantitative spectral studies (IR and UV–vis) establish the ready interconversion of the 6-coordinate O$_2$RuCl$_4$$^{2-}$ to the 5-coordinate analogue with a dissociation constant K = 5.3 × 10^{-3} M for chloride loss in dichloromethane. The octahedral structure of O$_2$RuCl$_4$$^{2-}$ is established by X-ray crystallography of the (Ph$_3$P)$_2$N$^+$ salt to consist of *trans*-dioxo ligands with the asymmetric (A$_{2u}$) stretching band at 830 cm^{-1} in the IR spectrum. [(Ph$_3$P)$_2$N$^+$]$_2$[O$_2$RuCl$_4$$^{2-}$]: space group $P\bar{1}$ (triclinic) with lattice constants a = 10.916 (2) Å, b = 12.378 (2) Å, c = 13.788 (2) Å, α = 105.65 (1)°, β = 93.16 (1)°, γ = 92.60 (1)°, and Z = 1. The coordinatively unsaturated trichloro derivative O$_2$RuCl$_3$$^-$ represents a rare example of a mononuclear dioxo complex whose solid-state structure is dependent on the counterion. Thus, the X-ray crystallography of the (Ph$_3$P)$_2$N$^+$ salt establishes a trigonal-bipyramidal structure of O$_2$RuCl$_3$$^-$ with the *cis*-dioxo ligands absorbing as a single, strong IR band at 882 cm^{-1}. [(Ph$_3$P)$_2$N$^+$][O$_2$RuCl$_3$$^-$]: space group $P2_1/n$ (monoclinic) with lattice constants a = 10.629 (4) Å, b = 15.636 (5) Å, c = 21.026 (7) Å, β = 99.60 (2)°, and Z = 4. The O$_2$RuCl$_3$$^-$ ion in the Ph$_4$P$^+$ salt is disordered between trigonal-bipyramidal and square-pyramidal geometries, which can be refined by using an occupancy ratio of 6:4 with R = 0.042 in the final refinement. The square-pyramidal component of O$_2$RuCl$_3$$^-$ is assigned with *trans*-dioxo ligands that account for the appearance of the unusual IR band at 891 cm^{-1} (together with the band at 878 cm^{-1}) in crystalline [O$_2$RuCl$_3$$^-$][Ph$_4P^+$] [tetragonal space group $P4/n$ with lattice constants a = 12.672 (2) Å, c = 7.788 (2) Å, and Z = 2]. The (Ph$_3$P)$_2$N$^+$, Ph$_4$P$^+$, Et$_4$N$^+$, and n-Bu$_4$N$^+$ salts of O$_2$RuCl$_3$$^-$ all show a single, sharp IR band at 885 cm^{-1} in solutions of dichloromethane or acetonitrile.

Introduction

Increasing interest accrues for oxometals as viable catalysts for oxygen atom transfer to various substrates.[1,2] Among metal

complexes, those of ruthenium are especially attractive since different oxoruthenium species have been identified with the high oxidation states IV–VIII.[3–9] Indeed, the ready availability of such

(1) Holm, R. H. *Chem. Rev.* **1987**, *87*, 1401.
(2) Sheldon, R. A.; Kochi, J. K. *Metal-Catalyzed Oxidation of Organic Compounds*; Academic: New York, 1981.

(3) Seddon, E. A.; Seddon, K. R. *The Chemistry of Ruthenium*; Elsevier: Amsterdam, 1984.
(4) Green, G.; Griffith, W. P.; Hollinshead, D. M.; Ley, S. V.; Schröder, M. *J. Chem. Soc., Perkin Trans. 1* **1984**, 681.